

Stellar Radio Astronomy

Probing Stellar Atmospheres from Protostars to Giants

Manuel Güdel

Paul Scherrer Institut, Würenlingen & Villigen, CH-5232 Villigen PSI, Switzerland
e-mail: guedel@astro.phys.ethz.ch

KEYWORDS: radio stars, coronae, stellar winds, high-energy particles, non-thermal radiation, magnetic fields

ABSTRACT: Radio astronomy has provided evidence for the presence of ionized atmospheres around almost all classes of non-degenerate stars. Magnetically confined coronae dominate in the cool half of the Hertzsprung-Russell diagram. Their radio emission is predominantly of non-thermal origin and has been identified as gyrosynchrotron radiation from mildly relativistic electrons, apart from some coherent emission mechanisms. Ionized winds are found in hot stars and in red giants. They are detected through their thermal, optically thick radiation, but synchrotron emission has been found in many systems as well. The latter is emitted presumably by shock-accelerated electrons in weak magnetic fields in the outer wind regions. Radio emission is also frequently detected in pre-main sequence stars and protostars, and has recently been discovered in brown dwarfs. This review summarizes the radio view of the atmospheres of non-degenerate stars, focusing on energy release physics in cool coronal stars, wind phenomenology in hot stars and cool giants, and emission observed from young and forming stars.

Eines habe ich in einem langen Leben gelernt, nämlich, dass unsere ganze Wissenschaft, an den Dingen gemessen, von kindlicher Primitivität ist - und doch ist es das Kostlichste, was wir haben.

One thing I have learned in a long life: that all our science, measured against reality, is primitive and childlike - and yet it is the most precious thing we have.

A. Einstein 1951, in a letter to H. Mühsam, Einstein Archive 36-610

1 INTRODUCTION

Stellar radio astronomy has matured over the past two decades, driven in particular by discoveries made with the largest and most sensitive radio interferometers. Radio emission is of great diagnostic value as it contains telltale signatures not available from any other wavelength regime. Some of the detected radio emission represents the highest-energy particle populations (MeV electrons) yet accessible on stars, the shortest (sub-second) detectable time scales of variability and energy release, and probably refers most closely to the primary energy release responsible for coronal heating. This review is to a large extent devoted to demonstrating the ubiquity of high-energy processes in stars as revealed by radio diagnostics.

Stellar radio sources include thermal and non-thermal magnetic coronae, transition regions and chromospheres, stars shedding winds, colliding-wind binaries, pre-main sequence stars with disks and radio jets, and embedded young objects visible almost exclusively by their radio and

millimeter-wave emission. Most recent additions to the zoo of objects are brown dwarfs, and with the increasingly blurred transition from stars to brown dwarfs to giant planets like Jupiter and Saturn, even the magnetospheres of the latter may have to be considered a manifestation of magnetic activity in the widest sense. To keep the discussion somewhat focused, this paper concentrates on physical processes in magnetic coronae, but includes, in a more cursory way, atmospheres of young and forming stars and winds of hot stars. We do not address in detail the large phenomenology of extended and outflow-related sources such as radio jets, HII regions, masers, Herbig-Haro objects, and the diverse millimeter/submillimeter phenomenology, e.g., molecular outflows and dust disks. Compact stellar objects (white dwarfs, neutron stars, black holes) are not considered here.

Inevitably - and fortunately - much of the knowledge gained in stellar astronomy is anchored in solar experience. The privilege of having a fine specimen - and even an exemplary prototype - next door is unique among various fields of extrasolar astrophysics, being shared since recently only by the related field of extrasolar planetary astronomy. Detailed solar studies, even in-situ measurements of the solar wind, are setting high standards for studies of stellar atmospheres, with a high potential reward. Solar radio astronomy has been reviewed extensively in the literature. For detailed presentations, we refer to Dulk (1985) and Bastian et al. (1998).

The maturity of stellar radio astronomy is demonstrated by a number of review articles on various subjects; a non-exhaustive list for further reference includes André (1996), Bastian (1990, 1996), Bookbinder (1988, 1991), Dulk (1985, 1987), Güdel (1994), Hjellming (1988), Kuipers (1985, 1989a), Lang (1990, 1994), Lestrade (1997), Linsky (1996), Melrose (1987), Mullan (1985, 1989), Mutel (1996), Phillips (1991), Seaquist (1993), van den Oord (1996), and White (1996, 2000). A natural starting point for this review, even if not strictly adhered to, is Dulk's comprehensive 1985 Annual Review article that summarizes the pre- and early-Very Large Array view of stellar (and solar) radio emission. Meanwhile, two dedicated conferences, the first one in Boulder in 1984 (proceedings edited by Hjellming & Gibson 1985) and the second held in Barcelona in 1995 (proceedings edited by Taylor & Paredes 1996), provided a rich forum to discuss new developments; together, they beautifully illustrate the progress made over the past decades.

2 RADIO SURVEYS AND THE RADIO HERTZSPRUNG-RUSSELL DIAGRAM

Figure 1 presents a radio Hertzsprung-Russell Diagram (HRD) based on stellar radio detections between 1–10 GHz, reported in the catalog of Wendker (1995); for other examples, see White (1996, 2000). The luminosity is the logarithmic average of all reported detections. The accuracy of the location of some stars on the HRD is compromised by the limited quality of distance and color measurements, or in multiple systems, by the uncertain attribution of the radio emission to one of the components. Nevertheless, almost all of the usual features of an HRD are recovered, testifying to the importance and ubiquity of radio emission.

The many nearby M dwarfs in Figure 1 were among the first radio stars surveyed. The typically larger distances to earlier-type cool dwarfs made their discovery more of an adventure, but the samples now include late-type binaries, K stars, solar analog G stars, and a few F stars. Most radio-detected dwarf stars are strong X-ray sources and young, rapid rotators.

The cool half of the subgiant and giant area is dominated by the large and radio-strong sample of RS CVn and Algol-type close binaries. Other sources in this area include the vigorous coronal radio sources of the FK Com class, chromospheric radio sources, symbiotic stars and thermal-wind emitters. Additionally, a very prominent population of thermal or non-thermal sources

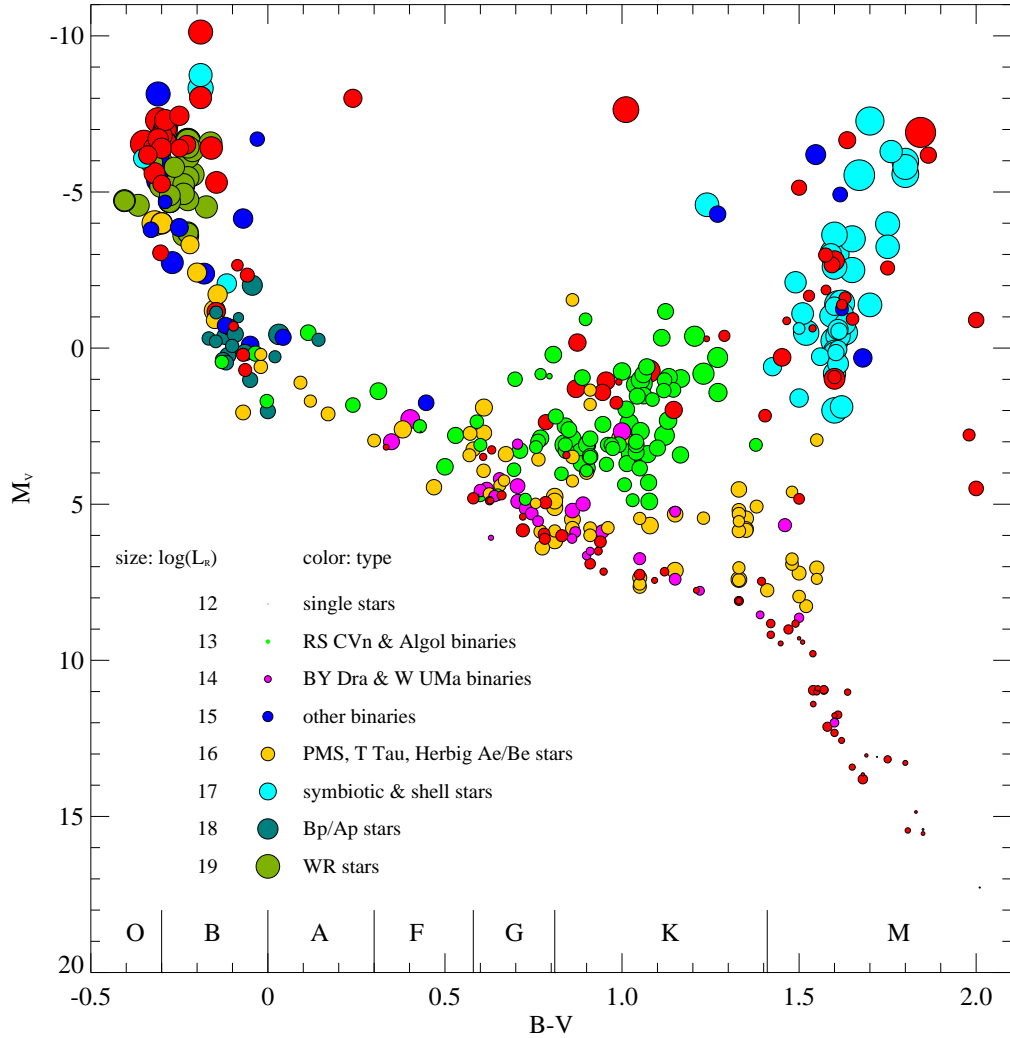


Figure 1: HR diagram showing 440 radio-detected stars.

just above the main sequence is made up of various classes of pre-main sequence stars, such as classical and weak-lined T Tauri stars.

Common to most cool star radio emitters is their non-thermal nature which, especially in its “quiescent” form, constitutes one of the most significant - and unexpected - discoveries in stellar radio astronomy, suggesting the presence of magnetic fields and high-energy electrons. Moving toward A-type stars on the HRD, one expects, and finds, a dearth of radio detections owing to the absence of magnetic dynamo action. However, this is also the region of the chemically peculiar Ap/Bp stars that possess strong magnetic fields and many of which are now known to be non-thermal radio sources as well. Some pre-main sequence Herbig Ae/Be stars in this area are also prominent radio emitters.

Finally, the hot-star region is heavily populated by luminous wind-shedding O and B stars and Wolf-Rayet (WR) stars, both classes showing evidence for either thermal or non-thermal radio emission.

3 THEORY OF RADIO EMISSION FROM STELLAR ATMOSPHERES

3.1 Elementary Formulae for Radiation and Particles

We summarize below some handy formulae that have become standard for most radio-stellar interpretational work (the interested reader is advised to consult the original literature as well). In thermodynamic equilibrium, the emissivity of a plasma of temperature T_{eff} , η_ν (in $\text{erg s}^{-1}\text{cm}^{-3}\text{Hz}^{-1}\text{sr}^{-1}$), and the absorption coefficient, κ_ν (in cm^{-1}) are related by Kirchhoff's law; for combined modes of polarization, for unity spectral index and a frequency $\nu \ll 10^{10}T_{\text{eff}}$ (ν in Hz, T_{eff} in K; Rayleigh-Jeans approximation):

$$\frac{\eta_\nu}{\kappa_\nu} = \frac{2kT_{\text{eff}}\nu^2}{c^2} \approx 3.1 \times 10^{-37} T_{\text{eff}} \nu^2. \quad (1)$$

Here, $k = 1.38 \times 10^{-16} \text{ erg K}^{-1}$ is the Boltzmann constant. The brightness temperature T_b is

$$T_b = \begin{cases} \tau T_{\text{eff}}, & \tau \ll 1 \\ T_{\text{eff}}, & \tau \gg 1 \end{cases} \quad (2)$$

with $\tau = \int \kappa d\ell$ being the optical depth along the line of sight ℓ . The spectral radio flux density S_ν then is

$$S_\nu = \frac{2kT_b\nu^2}{c^2} \frac{A}{d^2} \approx 0.1 \left(\frac{T_b}{10^6 \text{ K}} \right) \left(\frac{\nu}{1 \text{ GHz}} \right)^2 \left(\frac{r}{10^{11} \text{ cm}} \right)^2 \left(\frac{1 \text{ pc}}{d} \right)^2 \text{ mJy} \quad (3)$$

where A is the cross sectional source area perpendicular to the line of sight, and the approximation on the right-hand side is for a circular source with $A = \pi r^2$. In non-thermal astrophysical plasmas, electron volumetric number densities are often observed to follow a power-law form

$$n(\epsilon) = N(\delta - 1)\epsilon_0^{\delta-1}\epsilon^{-\delta} \quad [\text{cm}^{-3}\text{erg}^{-1}] \quad (4)$$

where $\epsilon = (\gamma - 1)m_e c^2$ is the kinetic particle energy, γ is the Lorentz factor, and $\delta > 1$ has been assumed so that N is the total non-thermal electron number density above ϵ_0 . A fundamental frequency of a plasma is its plasma frequency, given by

$$\nu_p \equiv \frac{\omega_p}{2\pi} = \left(\frac{n_e e^2}{\pi m_e} \right)^{1/2} \approx 9000 n_e^{1/2} \quad [\text{Hz}]. \quad (5)$$

Here, $m_e = 9.1 \times 10^{-28} \text{ g}$ is the electron rest mass, $e = 4.8 \times 10^{-10} \text{ esu}$ is the electron charge, and n_e is the total electron number density (cm^{-3}).

3.2 Bremsstrahlung

A thermal plasma emits free-free emission (bremsstrahlung) across the electromagnetic spectrum. For cosmic abundances, the absorption coefficient is then approximately given by (in the usual units; $T \equiv T_{\text{eff}}$, mix of 90% H and 10% He; upper equation for singly ionized species, lower equation for fully ionized plasma, and $\nu \gg \nu_p$; Dulk 1985, Lang 1999):

$$\kappa_\nu \approx 0.01 n_e^2 T^{-3/2} \nu^{-2} \times \begin{cases} \ln(5 \times 10^7 T^{3/2}/\nu), & T \lesssim 3.2 \times 10^5 \text{ K} \\ \ln(4.7 \times 10^{10} T/\nu), & T \gtrsim 3.2 \times 10^5 \text{ K} \end{cases} \quad (6)$$

and the emissivity η_ν follows from equation 1. Optically thick bremsstrahlung shows a ν^2 dependence, whereas optically thin flux is nearly independent of ν . A homogeneous optically thin magnetized source is polarized in the sense of the magnetoionic x-mode, whereas an optically thick source is unpolarized (Dulk 1985).

3.3 Gyromagnetic Emission

Electrons in magnetic fields radiate gyromagnetic emission. The gyrofrequency in a magnetic field of strength B is

$$\nu_c \equiv \frac{\Omega_c}{2\pi} = \frac{eB}{2\pi m_e c} \approx 2.8 \times 10^6 B \text{ [Hz]} \quad (7)$$

where $c = 3 \times 10^{10} \text{ cm s}^{-1}$ is the speed of light, and the magnetic field strength B is given in Gauss. The relativistic gyrofrequency is $\nu_{c,\text{rel}} = \nu_c/\gamma$. For large pitch angles, spectral power is predominantly emitted around a harmonic s with

$$\nu_{\text{max}} = s\nu_{c,\text{rel}} \approx \gamma^3 \nu_{c,\text{rel}} \approx 2.8 \times 10^6 B \gamma^2 \text{ [Hz]}. \quad (8)$$

Depending on γ , the emission is termed *gyroresonance* or *cyclotron* emission ($s < 10$, $\gamma \approx 1$, non-relativistic, typically thermal electrons), *gyrosynchrotron* ($s \approx 10 - 100$, $\gamma \lesssim 2 - 3$, mildly relativistic electrons), or *synchrotron* emission ($s > 100$, $\gamma \gg 1$, relativistic electrons). Because relativistic effects play an increasingly important role in increasing s , the fundamental properties (e.g., directivity, bandwidth, polarization) change between the three categories of gyromagnetic emission. The total power emitted by an electron is (Lang 1999)

$$P = 1.6 \times 10^{-15} \beta^2 \gamma^2 B^2 \sin^2 \alpha \text{ [erg s}^{-1}\text{]} \quad (9)$$

where $\beta = v/c = (1 - \gamma^{-2})^{1/2}$ and α is the pitch angle of the electron.

Simplified approximate expressions for separate magnetoionic modes of gyromagnetic emission have been given by Dulk & Marsh (1982), Robinson & Melrose (1984), and Klein (1987). For stellar observations, the angle θ between the line of sight and the magnetic field is often unknown and should be averaged. We give handy, simplified expressions for η_ν , κ_ν , the turnover frequency ν_{peak} , and the degree of circular polarization r_c derived from Dulk (1985) for $\theta = \pi/3$, with exponents for the model parameters B, N, T , and the characteristic source scale along the line of sight, L . For more comprehensive expressions, we refer to the original work by Dulk & Marsh (1982) and Dulk (1985).

Gyroresonance emission: If s is the harmonic number, $s^2 T \ll 6 \times 10^9 \text{ K}$ and $\nu \gtrsim \nu_c$, then for each magnetoionic mode (for unity refractive index),

$$\kappa_\nu(s) = 1020(1 \pm 0.5)^2 \frac{n_e}{\nu T^{1/2}} \frac{s^2}{s!} \left(\frac{s^2 T}{1.6 \times 10^{10}} \right)^{s-1} \exp \left[-\frac{(1 - s\nu_c/\nu)^2}{8.4 \times 10^{-11} T} \right] \quad (10)$$

$$\eta_\nu(s) = \frac{kT\nu^2}{c^2} \kappa_\nu(s) \quad (11)$$

(for the x-mode, and marginally for the o-mode, see Dulk 1985) where n_e is the ambient electron density. Properties: Emission is strongly concentrated in emission “lines” at harmonic frequencies $s\nu_c$, and κ_ν depends on the magnetoionic mode (lower sign for o-mode, upper sign for x-mode). The emission at a given harmonic comes from a layer of constant B with a thickness $L = 2\Lambda_B \beta_0 \cos \theta \approx \Lambda_B \beta_0$ determined by the magnetic scale length $\Lambda_B = B/\nabla B$ and $\beta_0 \equiv [kT/(m_e c^2)]^{1/2} \approx 1.3 \times 10^{-5} T^{1/2}$.

Gyrosynchrotron Emission from a Thermal Plasma: If $10^8 \lesssim T \lesssim 10^9$ K and $10 \lesssim s \lesssim 100$, then for the x-mode (and r_c for $\tau \ll 1$)

$$\kappa_\nu \approx 21 n_e T^7 B^9 \nu^{-10} \quad (12)$$

$$\eta_\nu \approx 3.2 \times 10^{-36} n_e T^8 B^9 \nu^{-8} \quad (13)$$

$$\nu_{\text{peak}} \approx 1.3 (n_e L / B)^{0.1} T^{0.7} B \quad (14)$$

$$r_c \approx 2.9 \times 10^4 T^{-0.138} (\nu / B)^{-0.51}. \quad (15)$$

Properties: The spectral power is $\propto \nu^2$ on the optically thick side, but $\propto \nu^{-8}$ on the optically thin side of the spectrum for a homogeneous source.

Gyrosynchrotron Emission from a Power-Law Electron Distribution: For isotropic pitch angle electron distributions according to equation 4, with $\epsilon_0 = 10$ keV = 1.6×10^{-8} erg, $2 \lesssim \delta \lesssim 7$, and $10 \lesssim s \lesssim 100$, and for the x-mode (and r_c for $\tau \ll 1$)

$$\kappa_\nu \approx 10^{-0.47+6.06\delta} N B^{0.3+0.98\delta} \nu^{-1.3-0.98\delta} \quad (16)$$

$$\eta_\nu \approx 10^{-31.32+5.24\delta} N B^{-0.22+0.9\delta} \nu^{1.22-0.9\delta} \quad (17)$$

$$\nu_{\text{peak}} \approx 10^{3.41+0.27\delta} (NL)^{0.32-0.03\delta} B^{0.68+0.03\delta} \quad (18)$$

$$r_c \approx 10^{3.35+0.035\delta} (\nu / B)^{-0.51}. \quad (19)$$

Properties: Broad spectra with intermediate circular polarization degree on the optically thin side. Optically thick spectral power is approximately $\propto \nu^{5/2}$, and the optically thin side is a power law with an index $\alpha = 1.22 - 0.9\delta$ for a homogeneous source.

Synchrotron Emission from a Power-Law Electron Distribution (homogeneous and isotropic): For $\gamma \gg 1$, i.e., $s \gg 100$, in each of the magnetoionic modes

$$\kappa_\nu \approx 10^{5.89+1.72\delta} (\delta - 1) N B^{(\delta+2)/2} \nu^{-(\delta+4)/2} \quad (20)$$

$$\eta_\nu \approx 10^{-24.7+1.57\delta} (\delta - 1) N B^{(\delta+1)/2} \nu^{-(\delta-1)/2} \quad (21)$$

$$\nu_{\text{peak}} \approx \left[10^{11.77+3.44\delta} (\delta - 1)^2 N^2 L^2 B^{\delta+2} \right]^{1/(\delta+4)} \quad (22)$$

Properties: Continuous and broad spectrum, important harmonics $s \approx \gamma^3$. For a homogeneous, optically thin source, the degree of linear polarization is $r = (\delta + 1)/(\delta + 7/3)$. The optically thick (self-absorbed) spectral power is $\propto \nu^{5/2}$, and the optically thin side of the spectrum has a power-law spectral index of $\alpha = -(\delta - 1)/2$.

3.4 Coherent Emission

The brightness temperature of synchrotron emission is limited to $T_b \lesssim 10^{12}$ K by inverse Compton scattering (Kellermann & Pauliny-Toth 1969). If higher T_b is observed, then a coherent radiation mechanism should be considered. Two mechanisms have received most attention both for solar and stellar coherent bursts (for details, see Benz 2002):

Plasma radiation is emitted at the fundamental or the second harmonic of ν_p (equation 5; for propagation parallel to the magnetic field), or of the upper hybrid frequency $\nu_{\text{UH}} = (\nu_p^2 + \nu_c^2)^{1/2}$ (for perpendicular propagation, with $\nu_p > \nu_c$). It is thus a useful means to approximately determine the electron density in the source. It can account for high brightness temperatures

(up to 10^{18} K, Melrose 1989) and small bandwidth, and it is frequently observed in the Sun (Bastian et al. 1998) and in low-frequency stellar flares (Bastian 1990). Owing to increasing free-free absorption with increasing ν (because $n_e \propto \nu_p^2$ in equation 6), and possibly also owing to gyroresonance absorption in hot plasma, fundamental emission is best observed below 1 GHz, although in very-high temperature environments such as coronae of RS CVn binaries, the absorption is milder and the limitations are more relaxed (White & Franciosini 1995). The escape of fundamental emission is also alleviated in a highly structured medium with sharp gradients in density (Aschwanden 1987, Benz et al. 1992).

Electron cyclotron maser emission (Melrose & Dulk 1982, 1984) is emitted mostly at the fundamental and the second harmonic of ν_c (equation 7) and can therefore be used to determine the magnetic field strength in the source. The requirement for radiation propagation, $s\nu_c > \nu_p$, also sets an upper limit to the electron density in the source and along the line of sight to the observer. The cyclotron maser mechanism accounts for the observed high T_b ($\lesssim 10^{20}$ K for $s = 1$, $\lesssim 10^{16-17}$ K for $s = 2$), and polarization degrees up to 100%.

Other mechanisms have occasionally been proposed. For example, plasma maser emission from a collection of double layers was initially calculated by Kuijpers (1989b) and applied to highly polarized stellar flare emission by van den Oord & de Bruyn (1994).

3.5 Wind emission

Olson (1975), Panagia & Felli (1975), and Wright & Barlow (1975) calculated the radio spectrum of a spherically symmetric, ionized wind. If \dot{M} is the mass loss rate in units of $M_\odot \text{yr}^{-1}$, v the terminal wind velocity in km s^{-1} , d_{pc} the distance to the star in pc, and T the wind temperature in K, the optically thick radius is (we assume a mean atomic weight per electron of 1.2, and an average ionic charge of 1)

$$R_{\text{thick}} = 8 \times 10^{28} (\dot{M}/v)^{2/3} T^{-0.45} \nu^{-0.7} \quad [\text{cm}]. \quad (23)$$

Then, the following formulae apply (R_* in cm):

$$S_\nu = \begin{cases} 9 \times 10^{10} (\dot{M}/v)^{4/3} T^{0.1} d_{\text{pc}}^{-2} \nu^{0.6} [\text{mJy}], & \text{if } R_{\text{thick}} \geq R_* \\ 5 \times 10^{39} (\dot{M}/v)^2 T^{-0.35} R_*^{-1} d_{\text{pc}}^{-2} \nu^{-0.1} [\text{mJy}], & \text{if } R_{\text{thick}} < R_*. \end{cases} \quad (24)$$

3.6 Loss Times

Relativistic electrons in an ambient gas of density n_e lose energy by Coulomb collisions with the ions. The energy loss rate and the corresponding life time are (under typical coronal conditions; Petrosian 1985)

$$-\dot{\gamma}_{\text{coll}} = 5 \times 10^{-13} n_e \quad [\text{s}^{-1}], \quad \tau_{\text{coll}} = 2 \times 10^{12} \frac{\gamma}{n_e} \quad [\text{s}]. \quad (25)$$

For electrons in magnetic fields, the synchrotron loss rate and the life time are given by (Petrosian 1985, pitch angle = $\pi/3$)

$$-\dot{\gamma}_{\text{B}} = 1.5 \times 10^{-9} B^2 \gamma^2 \quad [\text{s}^{-1}], \quad \tau_{\text{B}} = \frac{6.7 \times 10^8}{B^2 \gamma} \quad [\text{s}]. \quad (26)$$

4 RADIO FLARES FROM COOL STARS

4.1 *Incoherent Flares*

Many radio stars have been found to be flaring sources, and a considerable bibliography on stellar radio flares is now available. As in the Sun, two principal flavors are present: incoherent and coherent radio flares. Incoherent flares with time scales of minutes to hours, broad-band spectra, and moderate degrees of polarization are thought to be the stellar equivalents of solar microwave bursts. Like the latter, they show evidence for the presence of mildly relativistic electrons radiating gyrosynchrotron emission in magnetic fields. Many flares on single F/G/K stars are of this type (Vilhu et al. 1993, Güdel et al. 1995b, 1998), as are almost all radio flares on M dwarfs above 5 GHz (Bastian 1990, Güdel et al. 1996a), on RS CVn binaries (Feldman et al. 1978, Mutel et al. 1985), on contact binaries (Vilhu et al. 1988), and on other active subgiants and giants although some of the latter perhaps stretch the “solar analogy” beyond the acceptable limit: The FK Com-type giant HD 32918 produced flare episodes lasting 2–3 weeks, with a radio luminosity of $6 \times 10^{19} \text{ erg s}^{-1} \text{ Hz}^{-1}$ (Slee et al. 1987b, Bunton et al. 1989). Its integrated microwave luminosity is thus about 1000 times larger than the total X-ray output of the non-flaring Sun!

4.2 *Coherent Radio Bursts*

Bursts that exhibit the typical characteristics of coherent emission (see “Coherent Emission,” above) probably represent stellar equivalents of metric and decimetric solar bursts that themselves come in a complex variety (Bastian et al. 1998). Some exceptionally long-lasting (~ 1 h) but highly polarized bursts require a coherent mechanism as well (examples in Lang & Willson 1986a, White et al. 1986, Kundu et al. 1987, Willson et al. 1988, and van den Oord & de Bruyn 1994). Coherent flares are abundant on M dwarfs at longer wavelengths (20 cm; Kundu et al. 1988, Jackson et al. 1989). There are also some interesting reports on highly polarized, possibly coherent bursts in RS CVn binaries (Mutel & Weisberg 1978, Brown & Crane 1978, Simon et al. 1985, Lestrade et al. 1988, White & Franciosini 1995, Jones et al. 1996, Dempsey et al. 2001). After many early reports on giant metric flares observed with single-dish telescopes (Bastian 1990), the metric wavelength range has subsequently been largely neglected, with a few notable exceptions (Kundu & Shevgaonkar 1988, van den Oord & de Bruyn 1994).

Coherent bursts carry profound information in high-time resolution light curves. Radio “spike” rise times as short as 5–20 ms have been reported, implying source sizes of $r < c\Delta t \approx 1500\text{--}6000$ km and brightness temperatures up to $T_b \approx 10^{16}$ K, a clear proof of the presence of a coherent mechanism (Lang et al. 1983, Lang & Willson 1986b, Güdel et al. 1989a, Bastian et al. 1990). Quasi-periodic oscillations were found with time scales of 32 ms to 56 s (Gary et al. 1982, Lang & Willson 1986b, Bastian et al. 1990), and up to ≈ 5 min during a very strong flare (Brown & Crane 1978, although this emission was proposed to be gyrosynchrotron radiation).

4.3 *Radio Dynamic Spectra*

If the elementary frequencies relevant for coherent processes, ν_p and ν_c , evolve in the source, or the radiating source itself travels across density or magnetic field gradients, the emission leaves characteristic traces on the $\nu - t$ plane, i.e., on dynamic spectra (Bastian et al. 1998). A rich phenomenology has been uncovered, including: a) short, highly polarized bursts with structures as narrow as $\Delta\nu/\nu = 0.2\%$ suggesting either plasma emission from a source of size $\sim 3 \times 10^8$ cm, or a cyclotron maser in magnetic fields of ~ 250 G (Bastian & Bookbinder 1987, Güdel et al.

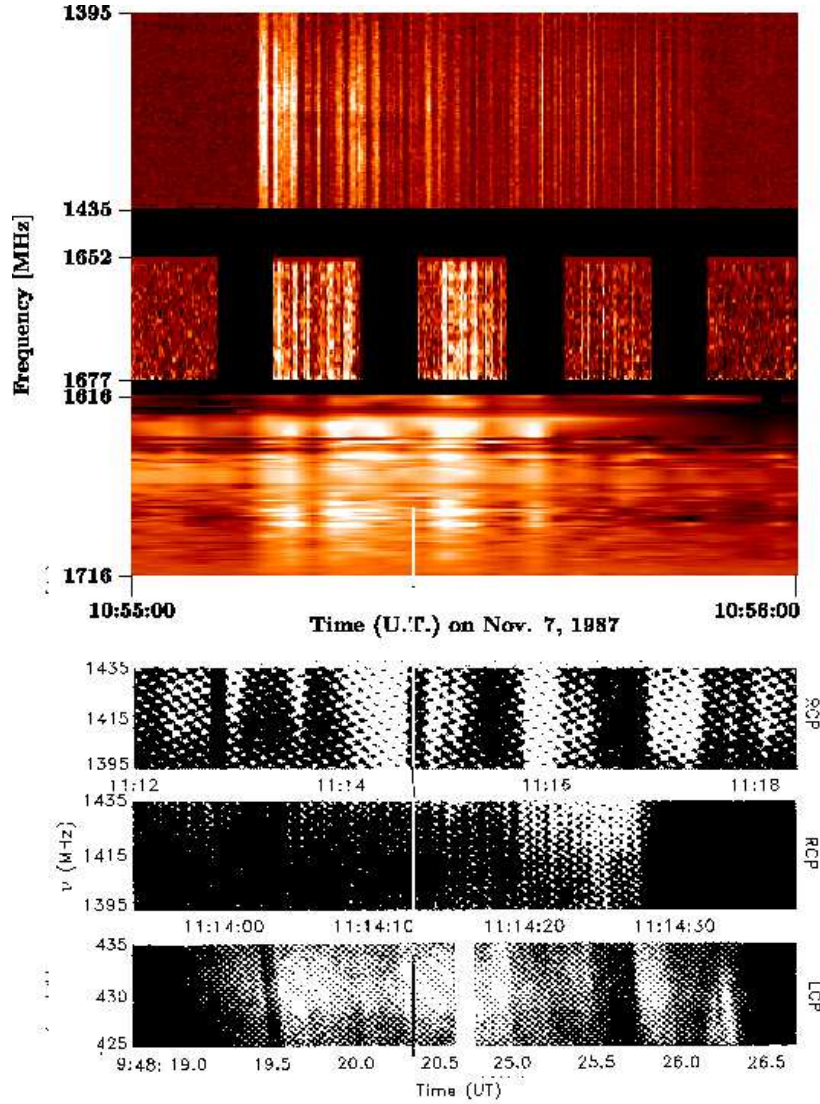


Figure 2: Gallery of radio dynamic spectra of M dwarf flares. Upper three panels show a flare on AD Leo, recorded with the Arecibo (top), Effelsberg (middle) and Jodrell Bank (bottom) telescopes in different wavelength ranges (see also Güdel et al. 1989a). Bottom three panels show flares on AD Leo (top and middle) and YZ CMi (bottom) observed at Arecibo (after Bastian et al. 1990, reproduced with permission of the AAS).

1989a, Bastian et al. 1990). b) Evidence for spectral structure with positive drift rates of 2 MHz s^{-1} around 20 cm wavelength, taken as evidence for a disturbance propagating “downward” in the plasma emission interpretation (Jackson et al. 1987); and c) in solar terminology, rapid broadband pulsations, “sudden (flux) reductions”, and positive and negative drift rates of $250\text{--}1000 \text{ MHz s}^{-1}$ (Bastian et al. 1990, Abada-Simon et al. 1994, 1997, see Figure 2).

The smallest spectral bandwidths were found to be in the 1% range for some bursts. Conservatively assuming a magnetic scale height of $\Lambda_B = 1R_*$, the source size can be estimated to be $r \approx (\Delta\nu/\nu)\Lambda_B \approx$ a few 1000 km, again implying very high T_b (Lang & Willson 1988a, Güdel et al. 1989a, Bastian et al. 1990).

5 QUIESCENT EMISSION FROM CORONAE OF COOL STARS

5.1 Phenomenology

The discovery of quiescent radio emission from magnetically active stars was one of the most fundamental and one of the least anticipated achievements in radio astronomy of cool stars because there simply is no solar counterpart. The Sun emits steady, full-disk, optically thick thermal radio emission at chromospheric and transition region levels of a few 10^4 K. However, one derives from equation 3 that such emission cannot be detected with present-day facilities, except for radiation from the very nearest stars, or giants subtending a large solid angle (see “Radio Emission from Chromospheres and Winds,” below). The radio luminosity of the corona caused by optically thin bremsstrahlung is proportional to the observed X-ray emission measure, but again the calculated radio fluxes are orders of magnitude below observed fluxes (Gary & Linsky 1981, Topka & Marsh 1982, Kuijpers & van der Hulst 1985, Borghi & Chiuderi Drago 1985, Massi et al. 1988, Güdel & Benz 1989, van den Oord et al. 1989). Obviously, another mechanism is in charge, and its characterization requires a proper description of the phenomenology.

Quiescent emission is best defined by the absence of impulsive, rapidly variable flare-like events. Common characteristics of quiescent emission are (i) slow variations on time scales of hours and days (Pallavicini et al. 1985, Lang & Willson 1986a, 1988a, Willson et al. 1988, Jackson et al. 1989), (ii) broad-band microwave spectra (Mutel et al. 1987, Güdel & Benz 1989), (iii) brightness temperatures in excess of coronal temperatures measured in X-rays (Mutel et al. 1985, Lang & Willson 1988a, White et al. 1989a), and often (iv) low polarization degrees (Kundu et al. 1988, Jackson et al. 1989, Drake et al. 1992). Occasionally, strong steady polarization up to 50% (Linsky & Gary 1983, Pallavicini et al. 1985, Willson et al. 1988, Jackson et al. 1989) or unexpectedly narrow-band steady emission (Lang & Willson 1986a, 1988a) is seen on M dwarfs. Quiescent emission has been reported at frequencies as low as 843 MHz (Vaughan & Large 1986, Large et al. 1989) and as high as 40 GHz (White et al. 1990).

5.2 Gyromagnetic Emission Mechanisms

Because active stars show high coronal temperatures and large magnetic filling factors (Saar 1990) that prevent magnetic fields from strongly diverging with increasing height, the radio optical depth can become significant at coronal levels owing to gyroresonance absorption (equation 10). Such emission is also observed above solar sunspots. The emission occurs at low harmonics of ν_c , typically at $s = 3 - 5$ (Güdel & Benz 1989, van den Oord et al. 1989, White et al. 1994). Rising spectra between 5 and 22 GHz occasionally observed on stars support such an interpretation (Cox & Gibson 1985) and imply the presence of $\sim 10^7$ K plasma in strong, kG magnetic fields (Güdel & Benz 1989; Figure 3). However, in most cases high-frequency fluxes are lower than predicted from a uniform, full-disk gyroresonance layer, constraining the filling factor of strong magnetic fields immersed in hot plasma. It is possible that the hot plasma resides in low- B field regions where the gyroresonance absorption is negligible, for example between strong fields from underlying active regions, or at large heights (White et al. 1994, Lim et al. 1996a). Uniform magnetic structures of ~ 600 G containing hot plasma can, on average, not reach out to beyond $1-2R_*$ on M dwarfs (Leto et al. 2000).

The gyroresonance mechanism cannot apply to lower-frequency radio emission, because the radius of the optically thick layer, still at $s = 3 - 5$, would have to be $> 3R_*$ for dMe stars. However, an extrapolation of the corresponding magnetic fields of more than 100 G down to photospheric levels would result in photospheric fields much stronger than observed (Gary & Linsky 1981, Topka & Marsh 1982, Linsky & Gary 1983, Pallavicini et al. 1985, Lang & Willson

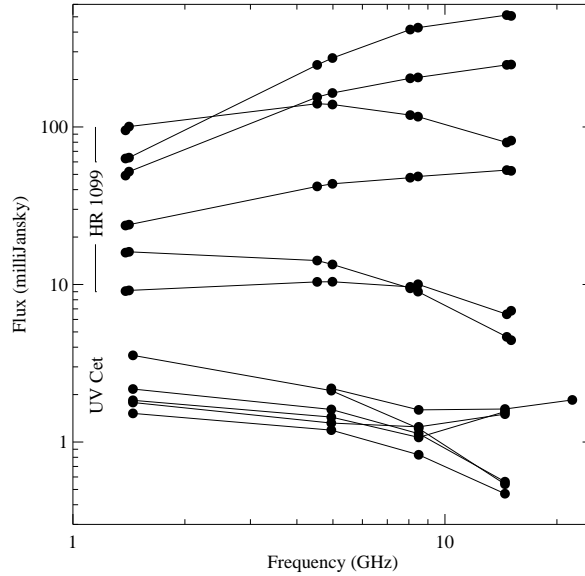


Figure 3: Radio spectra of the RS CVn binary HR 1099 (upper set) and of the dMe dwarf UV Cet (lower set) at different flux levels. The gently bent spectra are indicative of gyrosynchrotron emission, and the high-frequency part of U-shaped spectra for UV Cet has been interpreted as a gyroresonance component (HR 1099 spectra: courtesy of SM White).

1986a, Willson et al. 1988, Güdel & Benz 1989).

The only remedy is to allow for much higher T_{eff} . Then, the optically thick layer shifts to harmonics above 10, the range of gyrosynchrotron radiation, and the optically thick source sizes become more reasonable for M dwarfs, $R \approx R_*$ (Linsky & Gary 1983, Drake et al. 1989, 1992). For a thermal plasma, however, the spectral power drops like ν^{-8} at high frequencies (equation 13), far from the rather shallow $\nu^{-(0.3...1)}$ spectra of active stars (Massi & Chiuderi-Drago 1992; Figure 3). On the other hand, an optically thick thermal contribution requires strong magnetic fields (~ 200 G) over such large source areas that inferred photospheric magnetic fields again become unrealistically large (Kuijpers & van der Hulst 1985, Drake et al. 1992).

The situation is much more favorable for a non-thermal electron energy distribution such as a power law, analogous to distributions inferred for solar and stellar microwave flares (Kundu & Shevgaonkar 1985, Pallavicini et al. 1985). This model is supported by measured high brightness temperatures (Lestrade et al. 1984b, Mutel et al. 1985, Umana et al. 1991, Benz et al. 1995). Comprehensive spectral modeling suggests mildly relativistic electrons in ~ 100 G fields with power-law indices of $\delta \approx 2 - 4$, matching observed broad spectra with turnover frequencies in the 1 – 10 GHz range (White et al. 1989b, Slee et al. 1987a, 1988, Umana et al. 1998; Figure 3). The non-thermal model is now quite well established for many classes of active stars and provokes the question of how these coronae are continuously replenished with high-energy electrons.

Occasionally, steady narrow-band or strongly polarized coherent emission has been observed at low frequencies. An interesting possibility is large numbers of unresolved, superimposed coherent bursts (Pallavicini et al. 1985, Lang & Willson 1986a, 1988a, White & Franciosi 1995, Large et al. 1989).

6 RADIO FLARES AND CORONAL HEATING

6.1 *Is Quiescent Emission Composed of Flares?*

The question of the nature of stellar quiescent radio emission has defined one of the most fascinating aspects of stellar radio astronomy. A number of observations seem to suggest that flares play an important role - quiescent emission could simply be made up of unresolved flares. Inevitably, this question relates to the physics of coronal heating and the presence of X-ray coronae.

Very Long Baseline Interferometry (VLBI) studies of RS CVn binaries suggest that “flare cores” progressively expand into a large-scale magnetosphere around the star, radiating for several days (“flare remnant emission”). The electron distributions then evolve from initial power-law distributions as they are subject to collisional losses affecting the low-energy electrons and to synchrotron losses affecting the high-energy electrons. Time-dependent calculations predict rather flat spectra similar to those observed (Chiuderi Drago & Franciosini 1993, Franciosini & Chiuderi Drago 1995, Torricelli-Ciamponi et al. 1998).

6.2 *Microflaring at Radio Wavelengths*

Very long quiescent episodes with little flux changes impose challenges for flare-decay models. Limitations on the collisional losses (equation 25) require a very low ambient electron density (Massi & Chiuderi-Drago 1992). Frequent electron injection at many sites may be an alternative. Based on spectral observations, White & Franciosini (1995) suggest that the emission around 1.4 GHz is composed of a steady, weakly polarized broad-band gyrosynchrotron component plus superimposed, strongly and oppositely polarized, fluctuating plasma emission that is perceived as quasi-steady but that may occasionally evolve into strong, polarized flare emission (Simon et al. 1985, Lestrade et al. 1988, Jones et al. 1996, Dempsey et al. 2001; Figure 4).

RS CVn and Algol-type binaries also reveal significant, continuous gyrosynchrotron variability on time scales of ~ 10 – 90 minutes during $\sim 30\%$ of the time, with an increasing number of events with decreasing flux (Lefèvre et al. 1994). These flare-like events may constitute a large part of the quiescent gyrosynchrotron emission. However, “microbursts” or “nanoflares” with durations on the order of seconds to a few minutes are usually not detected at available sensitivities (Kundu et al. 1988, Rucinski et al. 1993) although Willson & Lang (1987) found some rapid variability on time scales between 30 s and 1 h that they interpreted as being due to variable absorption by thermal plasma.

6.3 *Radio Flares and the Neupert Effect*

The chromospheric evaporation scenario devised for many solar flares assumes that accelerated coronal electrons precipitate into the chromosphere where they lose their kinetic energy by collisions, thereby heating the cool plasma to coronal flare temperatures and evaporating it into the corona. The radio gyrosynchrotron emission from the accelerated electrons is roughly proportional to the injection rate of electrons, whereas the X-ray luminosity is roughly proportional to the accumulated energy in the hot plasma. To first order, one expects

$$L_R(t) \propto \frac{d}{dt} L_X(t), \quad (27)$$

a relation that is known as the “Neupert Effect” (Neupert 1968) and that has been well observed on the Sun in most impulsive and many gradual flares (Dennis & Zarro 1993). The search for

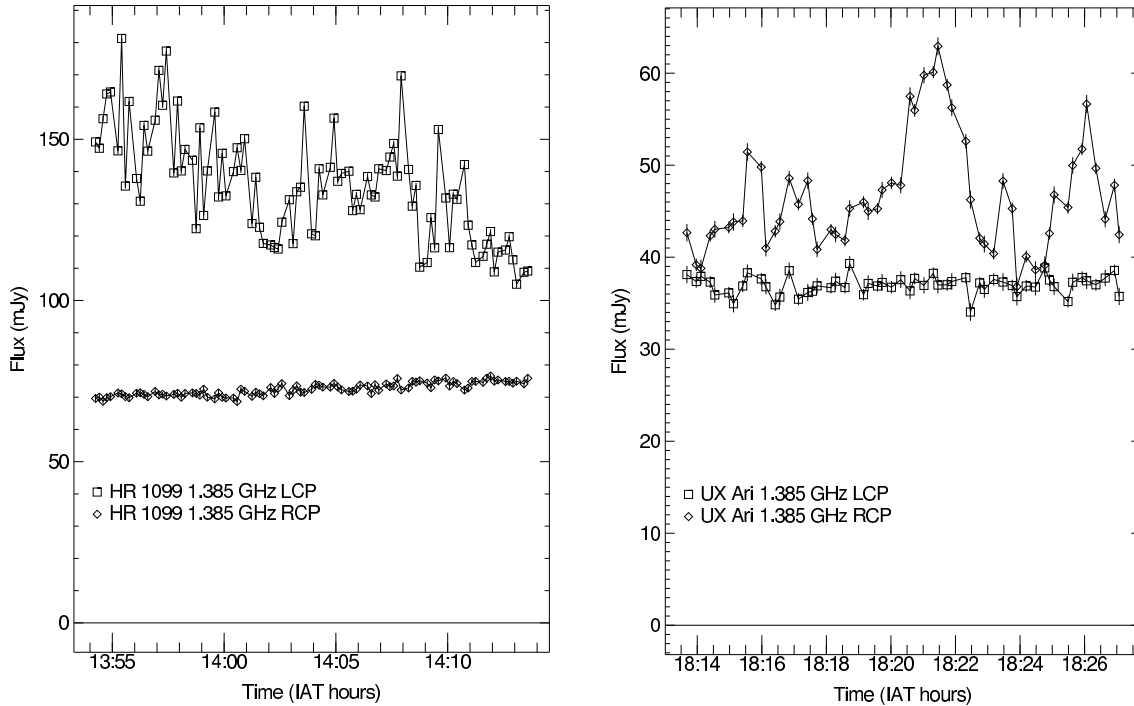


Figure 4: Light curves of HR 1099 (*left*) and UX Ari (*right*) obtained in the two senses of circular polarization. The brighter of the two polarized fluxes varies rapidly and has been interpreted as 100% polarized coherent emission superimposed on a gradually changing gyrosynchrotron component (White & Franciosini 1995; figures from SM White).

stellar equivalents has been a story of contradictions if not desperation (Figure 5). A first breakthrough came with simultaneous EUV (a proxy for X-rays) and optical observations (a proxy for the radio emission) of a flare on AD Leo (Hawley et al. 1995) and radio + X-ray observations of flares on UV Cet (Güdel et al. 1996a; Figure 5a). The latter revealed a relative timing between the emissions that is very similar to solar flares. Also, the energy ratios seen in non-thermal and thermal emissions are similar to solar analogs but, perhaps more interesting, they are also similar to the corresponding ratio for the quiescent losses. These observations suggest that high-energy particles are the ultimate cause for heating through chromospheric evaporation not only in flares, but also in the “quiescent” state. In retrospect, further suggestive examples of the Neupert effect can be found in the published literature, most notably in Vilhu et al. (1988), Stern et al. (1992), Brown et al. (1998), or Ayres et al. (2001).

It is important to note that the Neupert effect is observed neither in each solar flare (50% of solar gradual flares show a different behavior; Dennis & Zarro 1993), nor in each stellar flare. Stellar counter-examples include an impulsive optical flare with following gradual radio emission (van den Oord et al. 1996), gyrosynchrotron emission that peaks after the soft X-rays (Osten et al. 2000), and an X-ray depression during strong radio flaring (Güdel et al. 1998). Note also that complete absence of correlated flaring has been observed at radio and UV wavelengths (e.g., Lang & Willson 1988b).

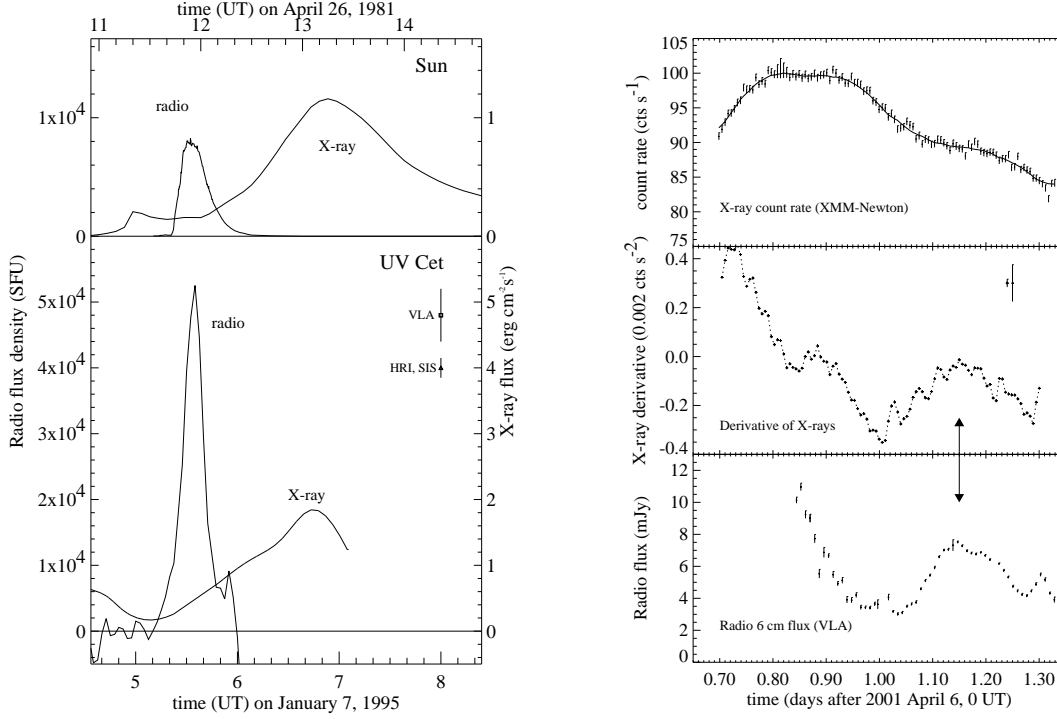


Figure 5: *Left*: Neupert effect seen in an M dwarf star, compared with a solar example in the upper panel (Güdel et al. 1996a). *Right*: Neupert effect seen in an RS CVn binary during a large flare (Güdel et al. 2002).

6.4 The Correlation between Quiescent Radio and X-Ray Emissions

Radio detections are preferentially made among the X-ray brightest stars (White et al. 1989a), a result that is corroborated by new, unbiased all-sky surveys (Helfand et al. 1999). For RS CVn and Algol binaries, one finds a correlation between the radio and X-ray luminosities, $L_R \propto L_X^{1.0-1.3}$ (Drake et al. 1986, 1989, 1992, Fox et al. 1994, Umana et al. 1998), whereas for late-type dwarfs, a rather tight linear correlation appears to apply (Güdel et al. 1993). In fact, several classes of active stars and solar flares follow a similar relation. Overall, for 5–8 GHz emission,

$$L_X/L_R \approx 10^{15 \pm 1} \text{ [Hz]} \quad (28)$$

(Güdel & Benz 1993, Benz & Güdel 1994; Figure 6). Phenomenologically, the relation simply suggests that both radio and X-ray emissions are activity indicators that reflect the level of magnetic activity. The most straightforward physical model, proposed by Drake et al. (1989, 1992), assumes that hot plasma emits both thermal X-rays and non-thermal gyrosynchrotron radiation, but this model predicts steep ($\propto \nu^{-8}$) optically thin spectra that are not observed.

Chiuderi Drago & Franciosini (1993) argued that the build-up of magnetic energy in magnetic loops is $\propto B^2$ and proportional to the gradient of the turbulent velocity (assumed to be similar in all stars). Since most of the energy in the magnetic fields is eventually radiated away in X-rays, $L_X \propto B^2 V$, where V is the source volume. A power-law electron population in the same loop emits optically thin radio radiation as $L_R \propto B^{-0.22+0.9\delta} V$ for given ν (equation 17). Therefore, $L_R \propto L_X^{0.45\delta-0.11} V^{1.11-0.45\delta}$. For $\delta = 3$, the dependence on V is small and $L_R \propto L_X^{1.24}$, close to

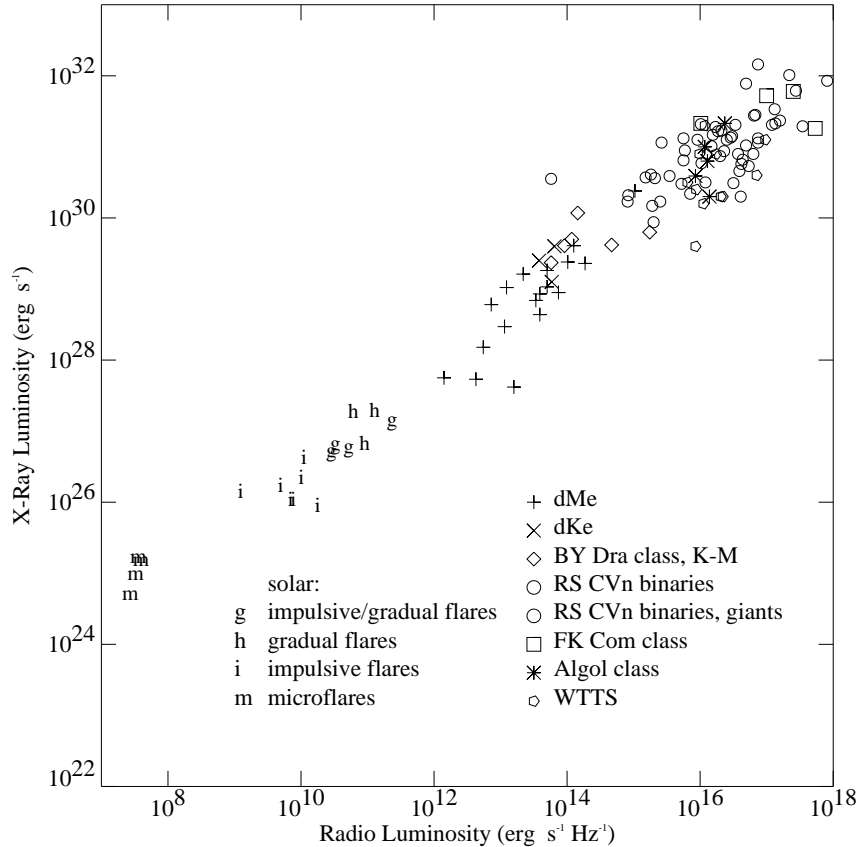


Figure 6: Correlation between quiescent radio and X-ray luminosities of magnetically active stars (symbols) and solar flares (letters; after Benz & Güdel 1994).

the reported relations.

If the quiescent emission is made up of numerous solar-like coronal flares, then the high-energy particles carry their energy downward to heat chromospheric plasma. For a steady-state situation in which the electron injection rate is balanced by an unspecified electron loss mechanism, one derives a relation between the synchrotron losses, the particle life time, and the energy losses in X-rays. Using the empirical correlation, Güdel & Benz (1993) estimated an electron life time that indeed corresponds quite well to the observed radio variability time scales. Holman (1985, 1986), and Airapetian & Holman (1998) presented detailed model calculations for the alternative situation of simultaneous heating and particle acceleration in current sheets.

7 STELLAR MAGNETIC FIELDS

Stellar radio astronomy has provided invaluable information on stellar coronal magnetic fields not accessible by any other methods. We briefly describe a few principal results. Electron cyclotron maser emission can be used to estimate the field strength in the source region, namely in converging, lower-coronal fields. Because the radiation is emitted at the fundamental ($s = 1$)

or the second harmonic ($s = 2$) of the gyrofrequency, $B = \nu_{\text{Hz}}/(s \times 2.8 \times 10^6) \approx 250 - 500$ G (Güdel et al. 1989a, Bastian et al. 1990).

Coronal gyroresonance emission detected at 8–23 GHz is optically thick at harmonics $s = 3 - 5$ of ν_B (see “Gyromagnetic Emission Mechanisms,” above), hence $B = \nu_{\text{Hz}}/(s \times 2.8 \times 10^6) \approx 600 - 2070$ G in low-lying loops in active regions (Güdel & Benz 1989).

Large coronal sizes as seen by VLBI restrict field strengths to typically 10–200 G if the approximate dipolar extrapolation to the photosphere should not produce excessive surface field strengths (Benz et al. 1998, Mutel et al. 1998, Beasley & Güdel 2000).

Very high synchrotron brightness temperatures T_b constrain, together with the power-law index δ , the characteristic harmonic numbers s and therefore the field strength (Dulk & Marsh 1982). Lestrade et al. (1984a, 1988), Mutel et al. (1984, 1985), and Slee et al. (1986) found B between ≈ 5 G and several tens of G for RS CVn halo sources, and a few tens to several hundred G for the core. Further, the electron energy is $\epsilon = kT_b$ for optically thick emission, and $\epsilon > kT_b$ for optically thin emission. Equation 8 for synchrotron emission ($s \gg 1$) then implies

$$B \leq \frac{2\pi m_e^3 c^5 \nu}{e(m_e c^2 + kT_b)^2} \approx 3.6 \times 10^{-7} \frac{\nu}{(1 + 1.7 \times 10^{-10} T_b)^2} \text{ [G]} \quad (29)$$

where the $<$ sign applies for optically thin emission. Alternatively, from Dulk & Marsh (1982) one finds for gyrosynchrotron emission $T_b \leq T_{\text{eff}} = 10^{6.15-0.85\delta} (\nu/B)^{0.5+0.085\delta}$. Such arguments lead to field strengths of a few tens to a few hundred G in RS CVn binaries (Mutel et al. 1985, Lestrade et al. 1988).

The synchrotron turnover frequency ν_{peak} determines B through $B = 2.9 \times 10^{13} \nu_{\text{peak}}^5 \theta^4 S^{-2}$ where θ is the source diameter in arcsec, S is the radio flux density in mJy at ν_{peak} which is given in units of GHz here (Lang 1999, after Sligh 1963). For a typical RS CVn or dMe coronal source with a size of 1 milliarcsec (mas) as measured by VLBI, a turnover at $\nu_{\text{peak}} \approx 5$ GHz and a flux of 10 mJy, magnetic fields of up to a few hundred G are inferred. For dipolar active region gyrosynchrotron models, White et al. (1989b) derived $B \approx 150 \nu_{\text{peak}}^{1.3}$ (ν_{peak} in GHz), which again implies field strengths of several hundred G for turnover frequencies in the GHz range.

Full spectral modeling of the magnetic field strength B , the non-thermal particle density, the geometric size, and the electron power-law index δ can constrain some of these parameters. Umana et al. (1993, 1999) and Mutel et al. (1998) found $B \approx 10 - 200$ G in their models for core plus halo structures in Algol-type stars.

8 RADIO CORONAL STRUCTURE

8.1 Introduction

Although the photospheric filling factor of kG magnetic fields on the Sun is small, it can exceed 50% on late-type active stars. On the Sun, magnetic fields can rapidly expand above the transition region and thus drop below kG levels. On magnetically active stars, such divergence is prevented by adjacent magnetic flux lines so that strong magnetic fields may exist also at coronal levels. The effective scale height of the coronal magnetic field however also largely depends on the structure of the magnetic flux lines, i.e., on whether they are compact loops with short baselines, long loops connecting distant active regions, or large dipolar magnetospheres anchored at the stellar poles. This issue is unresolved. Arguments for small-scale coronal active regions as well as for star-sized global magnetospheres have been put forward (see discussions in White et al. 1989b, Morris et al. 1990, and Storey & Hewitt 1996).

8.2 Radio Eclipses and Rotational Modulation

Eclipses and rotational modulation offer reliable information on radio source geometries, but neither are frequently seen. The radio sources may be much larger than the eclipsing star, or they may not be within the eclipse zone. Complete absence of radio eclipses has, for example, been reported for AR Lac (Doiron & Mutel 1984), Algol (van den Oord et al. 1989, Mutel et al. 1998), and YY Gem (Alef et al. 1997). Positive detections include the Algol system V505 Sgr (Gunn et al. 1999) and the pre-cataclysmic system V471 Tau (Patterson et al. 1993, Lim et al. 1996c). The former surprisingly shows both a primary and a secondary eclipse although one of the components is supposed to be inactive. The authors suggested that a radio coronal component is located between the two stars, a conjecture that gives rise to interesting theoretical models such as diffusion of magnetic fields from the active to the inactive star (on unreasonably long time scales, however), or radio emission from the optically thin mass accretion stream (which is found to be too weak), or field shearing by the inactive companion. The radio emission of V471 Tau may originate from magnetic loops that extend to the white dwarf where they interact with its magnetic field (Lim et al. 1996c).

Radio rotational modulation is often masked by intrinsic variability (Rucinski 1992). Well-documented examples are the RS CVn binaries CF Tuc (Budding et al. 1999) for which Gunn et al. (1997) suggested the presence of material in the intrabinary region, and the RS CVn binary UX Ari, which appears to have radio-emitting material concentrated above magnetic spots on the hemisphere of the K subgiant that is invisible from the companion (Neidhöfer et al. 1993, Elias et al. 1995, Trigilio et al. 1998). The clearest main-sequence example is AB Dor, with two emission peaks per rotation seen repeatedly over long time intervals. Both peaks probably relate to preferred longitudes of active regions (Slee et al. 1986, Lim et al. 1992, Vilhu et al. 1993). The shape of the maxima suggests that the radiation is intrinsically directed in the source, which is plausible for synchrotron emission by ultrarelativistic electrons (Lim et al. 1994).

8.3 Very Long Baseline Interferometry

Interferometry at large baselines has long been a privilege of radio astronomy and has proven versatile for numerous applications (Mutel 1996). Various intercontinental Very Long Baseline Interferometry (VLBI) networks have been arranged, and dedicated networks such as the US Very Large Baseline Array (VLBA) or the UK MERLIN network are routinely available. Apart from astrometric applications with sub-mas accuracy (Lestrade et al. 1990, 1993, 1995, 1999, Guirado et al. 1997), VLBI provides coronal mapping at $\lesssim 1$ mas angular resolution.

One of the principal, early VLBI results for RS CVn and Algol-like binaries relates to evidence for a compact core plus extended halo radio structure of a total size similar to the binary system size (Mutel et al. 1984, 1985, Massi et al. 1988, Trigilio et al. 2001). Compact cores appear to be flaring sites, whereas halo emission corresponds to quiescent, low-level radiation, perhaps from decaying electrons from previous flares. There is evidence for non-concentric, moving, or expanding sources (Lestrade et al. 1988, Trigilio et al. 1993, Lebach et al. 1999, Franciosi et al. 1999, Lestrade et al. 1999).

Pre-main sequence stars are attractive VLBI targets. Although some sources are overresolved at VLBI baselines (Phillips et al. 1993), others have been recognized as components in close binaries such as HD 283447 (Phillips et al. 1996); but most of the nearby weak-lined T Tau stars (see “Evolution to the Main Sequence,” below) reveal radio structures as large as $10R_*$, indicative of extended, global, probably dipolar-like magnetospheres somewhat similar to those seen in RS CVn binaries (Phillips et al. 1991, André et al. 1992). Perhaps also related to youth,

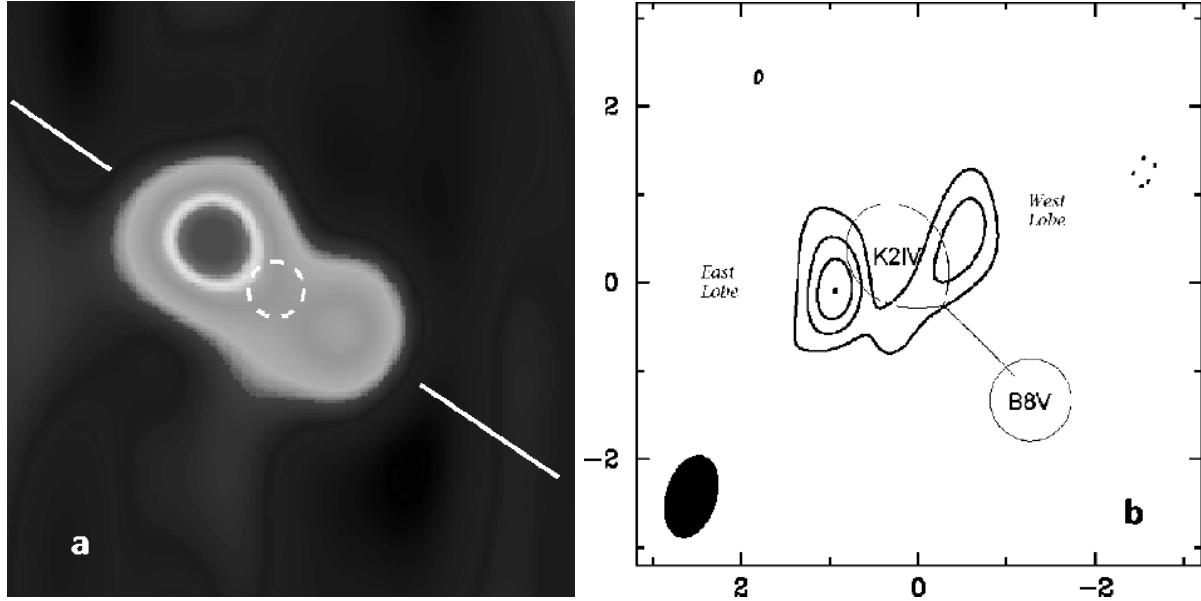


Figure 7: (a) VLBA image of the dMe star UV Cet; the two radio lobes are separated by about 1.4 mas, while the best angular resolution reaches 0.7 mas. The straight line shows the orientation of the putative rotation axis, assumed to be parallel to the axis of the orbit of UV Cet around the nearby Gl 65 A. The small circle gives the photospheric diameter to size, although the precise position is unknown (after Benz et al 1998). (b) VLBA image of the Algol binary. The most likely configuration of the binary components is also drawn. The radio lobes show opposite polarity (Mutel et al 1998; reproduced with permission of the AAS.)

magnetospheres around Bp/Ap stars have also been observed with VLBI and have strongly supported global magnetospheric models (Phillips & Lestrade 1988, André et al. 1991; see “Stars at the Interface Between Hot Winds and Coronae,” below).

VLBI techniques have been more demanding for single late-type dwarf stars, owing both to lower flux levels and apparently smaller coronal sizes. Some observations with mas angular resolutions show unresolved quiescent or flaring sources, thus constraining the brightness temperature to $T_b > 10^{10}$ K (Benz & Alef 1991, Benz et al. 1995), whereas others show evidence for extended coronae with coronal sizes up to several times the stellar size (Alef et al. 1997, Pestalozzi et al. 2000).

The dMe star UV Cet is surrounded by a pair of giant synchrotron lobes, with sizes up to 2.4×10^{10} cm and a separation of 4–5 stellar radii along the putative rotation axis of the star, suggesting very extended magnetic structures above the magnetic poles (Benz et al. 1998; Figure 7a). VLBA imaging and polarimetry of Algol reveals a similar picture with two oppositely polarized radio lobes separated along a line perpendicular to the orbital plane by more than the diameter of the K star (Mutel et al. 1998; Figures 7b, 8b). Global polarization structure is also suggested in UX Ari, supporting the view that the magnetic fields are large-scale and well ordered (Beasley & Güdel 2000).

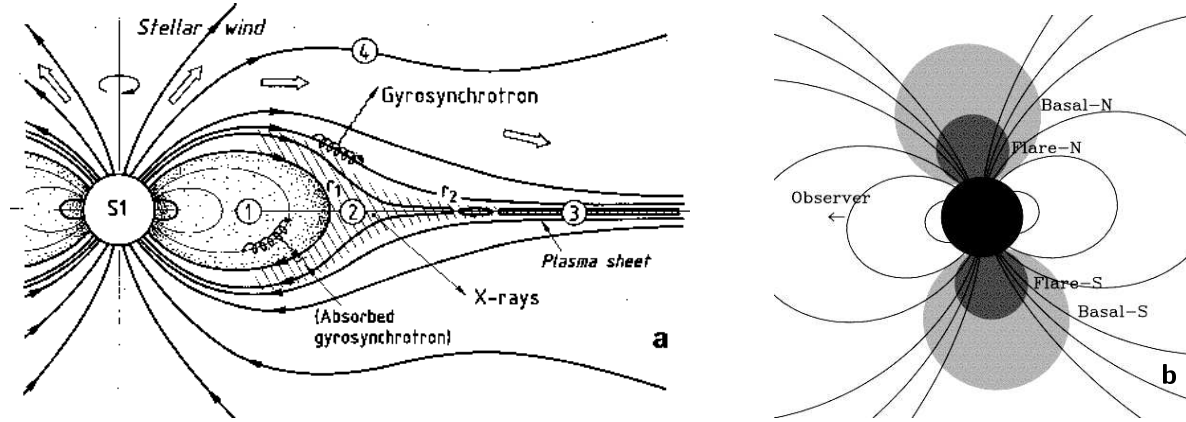


Figure 8: (a) Equatorial model for the magnetosphere of the young B star S1 in ρ Oph (André et al. 1988). (b) Sketch for radio emission from a global dipole consistent with the VLBI observation shown in Figure 7b (Mutel et al. 1998; reproduced with permission of the AAS.)

8.4 Magnetospheric Models

Quite detailed geometric models of large magnetospheres around RS CVn and Algol binaries, T Tau stars, and magnetic Bp/Ap stars have been designed based on VLBI results, radio spectra and polarization. Common to all is a global, dipole-like structure somewhat resembling the Earth's Van Allen belts (Figure 8a). Stellar winds escaping along magnetic fields draw the field lines into a current sheet configuration in the equatorial plane. Particles accelerated in that region travel back and are trapped in the dipolar-like, equatorial magnetospheric cavity. Variants of this radiation belt model, partly based on theoretical work of Havnes & Goertz (1984), have been applied to RS CVn binaries (Slee et al. 1987b, Morris et al. 1990, Jones et al. 1994, Storey & Hewitt 1996), in an optically thick version to Bp/Ap stars (Drake et al. 1987b, Linsky et al. 1992) and in an optically thin version to a young B star (André et al. 1988).

Such models are particularly well supported by polarization measurements in RS CVn binaries. For a given system, the polarization degree p at any frequency is anticorrelated with the luminosity, while the sense of polarization changes between lower and higher frequencies. For a stellar sample, p is inversely correlated with the stellar inclination angle such that low-inclination ("pole-on") systems show the strongest polarization degrees (Mutel et al. 1987, 1998, Morris et al. 1990).

When flares are in progress, the two-component core plus halo model appears to correctly describe radio spectral properties. Stronger magnetic fields of 80–200 G are inferred for the core and weaker fields of 10–30 G for the halo (Umana et al. 1993, 1999, Mutel et al. 1998, Trigilio et al. 2001). The frequency-dependent optical depth makes the source small at high frequencies (size $\approx R_*$, above 10 GHz) and large at small frequencies (size comparable to the binary system size at 1.4 GHz; Klein & Chiuderi-Drago 1987, Jones et al. 1995). This effect correctly explains the relatively flat, optically thick radio spectra seen during flares.

9 STELLAR ROTATION, BINARITY, AND MAGNETIC CYCLES

9.1 *Radio Emission and Stellar Rotation*

There is little doubt that rotation is largely responsible for the level of magnetic activity in cool stars. It is clearly the young, rapidly rotating stars or spun-up evolved stars in tidally interacting binaries that define the vast majority of radio-emitting cool stars detected to date. The rather peculiar class of FK Com stars, single giants with unusually short rotation periods of only a few days, are among the most vigorous emitters of gyrosynchrotron emission (Hughes & McLean 1987, Drake et al. 1990, Rucinski 1991, Skinner 1991), including extremely luminous and long flares (Slee et al. 1987b, Bunton et al. 1989). However, large surveys of RS CVn binary systems find at best a weak correlation between radio luminosity and rotation parameters (Mutel & Lestrade 1985, Morris & Mutel 1988, Caillault et al. 1988, Drake et al. 1989, 1992), and it may even depend on the optical luminosity class considered. Although Stewart et al. (1988) reported a trend of the form $L_R \propto R_*^{2.5} v^{2.5}$ (v is the equatorial velocity) for different luminosity classes, this result was later challenged (Drake et al. 1989) and may be related to using peak fluxes and flares. The absence of a correlation may be related to the coronal saturation regime known in X-rays (Vilhu & Rucinski 1983, Mutel & Lestrade 1985, White et al. 1989a): almost all radio-detected stars emit at the maximum possible and rotation-independent X-ray level - hence perhaps also at the maximum possible radio level. There is obviously a large potential for stellar radio astronomy in the less exotic regime below saturation!

Moving to tighter binary systems in which the components are in (near-)contact, we would expect magnetic activity to increase or at least to stay constant. This is however not the case. The radio emission of such systems is significantly weaker than that of RS CVn binaries or active single stars, a trend that is also seen at other wavelengths (Hughes & McLean 1984, Rucinski & Seaquist 1988, Vilhu et al. 1988). Possible physical causes include i) a reduced differential rotation, hence a weaker dynamo action (Beasley et al. 1993), ii) a shallower convection zone in contact binary systems, and iii) influence by the energy transfer between contacting stars (Rucinski 1995).

9.2 *Activity Cycles*

Radio polarization may be a telltale indicator for magnetic activity cycles on stars, analogous to the solar 11 year cycle (or 22 years, if the magnetic polarity reversal is considered). Long-term measurements in the Ca H&K lines (the HK project; Baliunas 1998) indicate the presence of activity cycles with durations of several years in low-activity stars, but irregular long-term variations on active stars. In any case, one would expect reversals of the dominant sense of polarization to accompany any of these quasi-cycles. The contrary is true, to an embarrassing level: After decades of monitoring, many active stars show a constant sign of radio polarization throughout, both in quiescence and during flares (Gibson 1983, White et al. 1986, Mutel et al. 1987, Kundu & Shevgaonkar 1988, Jackson et al. 1989, White & Franciosini 1995, Mutel et al. 1998) with few exceptions (Bastian & Bookbinder 1987, Willson et al. 1988, Lang 1990). This suggests the presence of some stable magnetospheric structures or a predominance of strong magnetic fields in one polarity. A concerted and ongoing effort to look for polarity reversals is negative at the time of this writing (S. White, private communication).

Perhaps the most convincing case yet reported in favor of a magnetic cycle is HR 1099 in which the average radio flux density correlates with the spot coverage, revealing a possible periodicity of 15–20 years (Umana et al. 1995). Massi et al. (1998) reported a surprisingly rapid quasi-periodicity in microwave activity ($P \approx 56 \pm 4$ days) and the accompanying sense of polarization

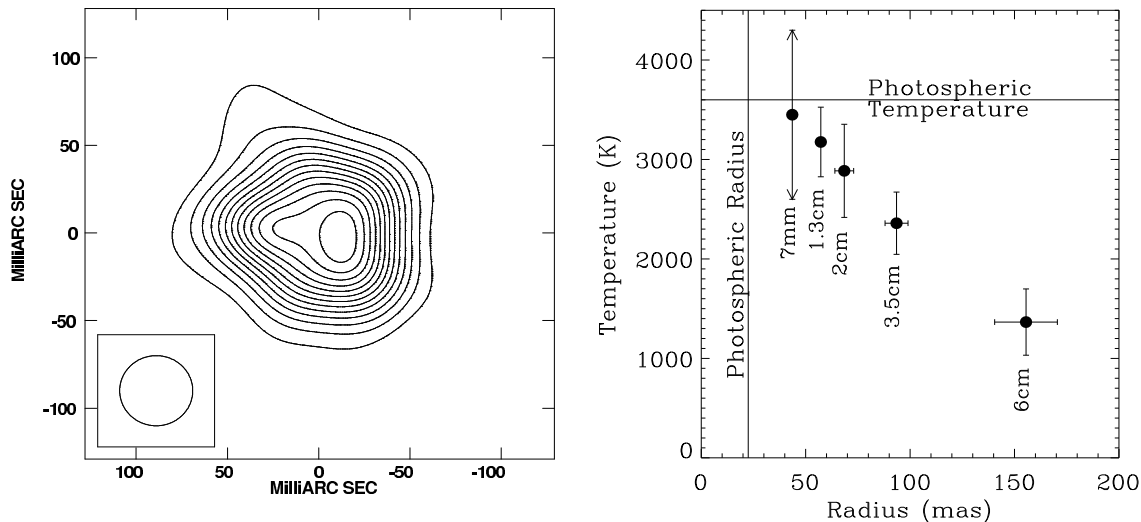


Figure 9: (a) Betelgeuse observed at 43 GHz. The radio photosphere of this star is resolved, with an angular resolution of 40 mas. (b) The atmospheric temperature of Betelgeuse as a function of radius, observed at different frequencies. (From Lim et al. 1998; reproduced with the permission of Nature.)

($P \approx 25$ days) in the RS CVn binary UX Ari. Whether such rapid oscillations are related to an internal magnetic dynamo cycle remains to be shown.

10 RADIO EMISSION FROM CHROMOSPHERES AND WINDS

10.1 Lower Atmospheres of Cool Stars

Stellar transition regions and chromospheres are expected to be radio sources as well (see “Quiescent Emission from Coronae of Cool Stars,” above). Among cool main-sequence stars, the slightly evolved mid-F star Procyon is the only such source in the solar vicinity detected to date (Drake et al. 1993). In the red giant area, however, outer atmospheres fundamentally change their characteristics. Chromospheres become as large as several stellar radii. Such sources are now well detected at radio wavelengths (Knapp et al. 1995) and spatially resolved (Skinner et al. 1997), albeit with some surprises. Because their outer atmospheres are optically thick at radio wavelengths, spatially resolved observations provide a direct temperature measurement. Reid & Menten (1997) inferred optically thick “radio photospheres” at about $2R_*$ but at subphotospheric/nonchromospheric temperatures. Indeed, contrary to chromospheric UV measurements, the radio-derived temperature in the nearby supergiant Betelgeuse is seen to drop systematically from optical-photospheric levels outward (Lim et al. 1998; Figure 9). This cool material completely dominates the outer atmosphere. The authors suggested that cool, photospheric material is elevated in giant convection cells; dust formation in this environment could then drive Betelgeuse’s outflow.

10.2 Winds from Cool Stars

Could dwarf stars lose mass by a substantial stellar wind (Doyle & Mathioudakis 1991, Mullan et al. 1992)? Such a wind, if (partially) ionized, would be a radio source. The very fact

that coronal radio flares are seen at GHz frequencies implies that the extended winds must be optically thin down to coronal heights, and this places stringent limits on the mass loss rate. Sensitive millimeter measurements and theoretical arguments have constrained such mass loss for M dwarfs to $\lesssim 10^{-13} M_{\odot} \text{ yr}^{-1}$ or $\lesssim 10^{-12} M_{\odot} \text{ yr}^{-1}$ for a 10^4 K or a 10^6 K wind, respectively (Lim & White 1996, Lim et al. 1996a, van den Oord & Doyle 1997), in agreement with upper limits derived from UV observations (Wood et al. 2001). Stringent upper limits to the radio emission of solar analogs also help confine the mass loss history of the Sun or solar-like stars (Drake et al. 1993, Gaidos et al. 2000). An upper limit to the mass loss during the Sun’s main-sequence life of 6% indicates that the Sun was never sufficiently luminous to explain the “Young Sun Paradox”, i.e., the suggestion that the young Sun was more luminous in early times given the apparently much warmer climate on Mars (Gaidos et al. 2000).

Winds become progressively more important toward the red giants, in particular beyond the corona-cool wind dividing line. Ionized-mass losses between $10^{-10} - 10^{-9} M_{\odot} \text{ yr}^{-1}$ are indicated, increasing toward cooler and more luminous stars (Drake & Linsky 1986). However, the surface mass loss flux is similar in all stars, in fact also similar to the solar wind mass loss flux. The coolest, late-M and C (super)giants still support massive winds, but the much weaker radio emission indicates that the ionization fraction drops by at least an order of magnitude compared to earlier M giants, i.e., their chromospheres must be cool, and their optical depth at radio wavelengths becomes small (Drake et al. 1987a, 1991a, Luttermoser & Brown 1992). The same holds for technetium-deficient S and M-S giants, although white dwarf companions of some of them may sufficiently ionize the outer atmosphere of the giant to become visible at radio wavelengths (Drake et al. 1991b). This latter mechanism is probably also relevant in the interacting “symbiotic binaries” that usually consist of a red giant and a white dwarf companion and that are radio sources with considerable luminosities. The white dwarf is sufficiently UV strong to ionize part of the cool-star wind (Seaquist et al. 1984, 1993, Taylor & Seaquist 1984, Seaquist & Taylor 1990). No appreciable radio emission is, however, detected from the similar class of G and K-type Barium stars (showing overabundances of Ba and other nuclear-processed elements), although they show evidence of white-dwarf companions (Drake et al. 1987c).

10.3 Ionized Winds and Synchrotron Emission from Hot Stars

Because OB and Wolf-Rayet stars shed strong ionized winds, they emit thermal-wind radio emission (equations 24). Some of the hot-star radio sources are very large and resolved by the VLA because the optically thick surface (equation 23) is located at hundreds of stellar radii. Under the assumption of a steady, spherically symmetric wind, wind mass-loss rates of $\dot{M} \approx 10^{-6} - 10^{-5} M_{\odot} \text{ yr}^{-1}$ are inferred for O and B stars (Scuderi et al. 1998), and $\dot{M} \approx 2 - 4 \times 10^{-5} M_{\odot} \text{ yr}^{-1}$ for WR stars (Bieging et al. 1982, Leitherer et al. 1995, 1997). The inferred mass-loss rate is closely correlated with the bolometric luminosity, $\log \dot{M} = (1.15 \pm 0.2) \log L + C$ (Scuderi et al. 1998), in good agreement with $H\alpha$ measurements. In the case of colliding wind binaries, the thermal radio emission can be further enhanced by contributions from the wind-shock zone (Stevens 1995). The radio emission level drops appreciably toward intermediate spectral classes of B, A, and F, probably owing to a steep decrease of the ionized mass loss (Drake & Linsky 1989).

It came as a surprise when several OB stars (Abbott et al. 1984, Bieging et al. 1989, Drake 1990, Contreras et al. 1996) and WR stars (Becker & White 1985, Caillault et al. 1985, Abbott et al. 1986, Churchwell et al. 1992, Chapman et al. 1999) were found to show non-thermal, synchrotron-like radio spectra, some of them associated with short-term variability (Persi et al. 1990). Up to 50% of the WR stars appear to be non-thermal sources, and this fraction is half

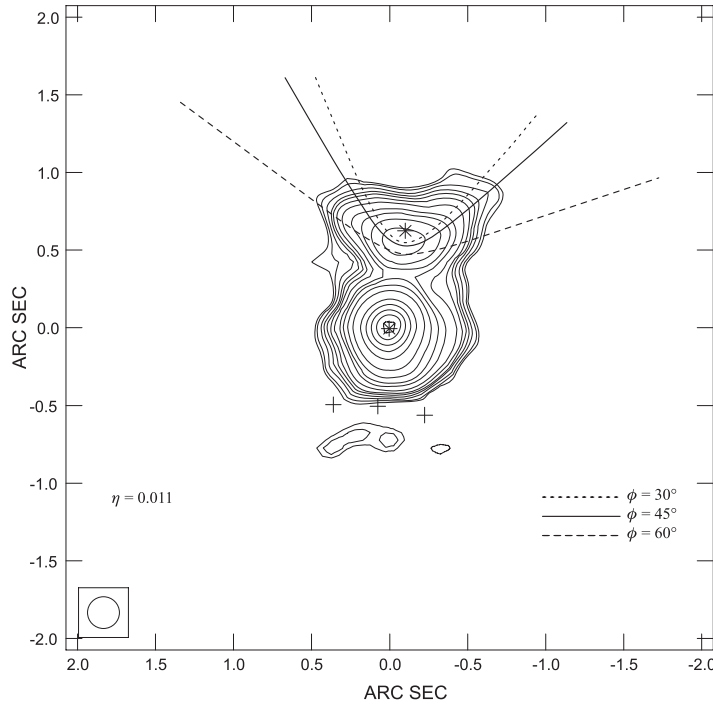


Figure 10: VLA map of the WR 147 system observed at 3.6 cm. Also shown are calculated model curves that follow the shock formed by the two-wind interaction (from Contreras & Rodríguez 1999; reproduced with the permission of the AAS).

as large for OB stars (Leitherer et al. 1997, Chapman et al. 1999, Dougherty & Williams 2000). Hot stars are not thought to produce magnetic fields via a dynamo. Moreover, because the wind is optically thick to radio emission out to hundreds of stellar radii, the non-thermal component must originate at such large distances as well. A coronal model should therefore not apply although highly variable radio emission and a poor correlation with X-ray behavior may suggest that magnetic fields play a role in the structuring of the winds (Waldron et al. 1998). Viable alternatives include synchrotron emission from electrons accelerated in shocks of unstable winds of single stars (White 1985, Caillault et al. 1985), in colliding-wind shocks in massive binaries (Eichler & Usov 1993), and in the interaction zone between the thermal wind and a previously ejected shell (Luminous Blue Variable phase; Leitherer et al. 1997). Magnetic fields inferred for the photospheric level are of order 1 Gauss (Bieging et al. 1989, Phillips & Titus 1990), and up to 50 G in synchrotron envelope models (Miralles et al. 1994).

Shocks are attractive features as they can accelerate electrons by the first-order Fermi mechanism, with a predicted electron energy power-law index $\delta = 2$ (Bell 1978). Skinner et al. (1999), however, found a significant deviation from this model for a colliding-wind binary but successfully interpreted their radio spectra with an absorbed synchrotron spectrum from a quasi-monoenergetic electron population. The origin and stability of such a population are unclear. The colliding-wind model found strong support when it became evident that most non-thermal sources are indeed binaries (Dougherty & Williams 2000) and that the non-thermal sources are located between the two stars, separate from the wind (Moran et al. 1989, Churchwell et al. 1992, Dougherty et al. 1996, 2000, Williams et al. 1997, Chapman et al. 1999). Convincing evidence

for colliding winds is available for WR 146 (Dougherty et al. 2000), Cygnus OB2 No 5 (Contreras et al. 1997), and WR 147 that all show a thermal source coincident with the WR star and a separate bow-shock shaped non-thermal source in the wind collision zone close to a lower-mass companion (Figure 10, Contreras & Rodríguez 1999). If the stars are in a strongly eccentric orbit, the wind-shock zone between two stellar components can enter the thermal-wind radio photosphere and become absorbed, thus producing strong long-term variability of the radio flux (Williams et al. 1990, 1992, 1994, White & Becker 1995, Setia Gunawan et al. 2000). Further long-term synchrotron variability may be caused by long-term modulation in the magnetic field along the orbit, whereas short-term (\sim daily) variability may be due to clumps in the wind that arrive at the shock (Setia Gunawan et al. 2000).

The rather inhomogeneous class of Be stars shows evidence for very large ($\sim 100R_*$) high-density outflowing disks that have been probed at radio wavelengths. Steeply increasing radio spectra and some flux variability are characteristic, but there is considerable debate on the source geometry (Taylor et al. 1987, 1990, Drake 1990, Dougherty et al. 1991).

There have been a number of interferometric observations of non-thermal sources among hot stars. Source sizes of order $100R_*$, exceeding the size of the optically thick surface of the thermal wind, have been measured. They imply brightness temperatures up to at least 4×10^7 K and thus further support the non-thermal interpretation (Felli et al. 1989, 1991, Felli & Massi 1991, Phillips & Titus 1990).

11 STAR FORMATION AND THE SOLAR-STELLAR CONNECTION

11.1 Radio Emission from Low-Mass Young Stellar Objects

Large numbers of visible T Tau stars and embedded infrared sources in star forming regions are strong radio sources (Garay et al. 1987, Felli et al. 1993). Schematically, pre-main sequence evolution is thought to proceed through four consecutive stages with progressive clearing of circumstellar material (Shu et al. 1987): i) Cold condensations of infalling molecular matter, forming a hydrostatic low-luminosity protostellar object, with the bulk mass still accreting (“Class 0 source”). ii) Formation of a deeply embedded protostar (“Class I source”) through further accretion via a massive accretion disk, associated with strong polar outflows. iii) The “classical T Tau” (CTT, “Class II”) phase with an optically visible star accompanied by a thick accretion disk, a weak outflow, and possibly a weakly ionized wind; and iv) the “weak-lined T Tau” (WTT, “Class III”) phase at which disk and circumstellar material have largely been dissipated, and the star approaches the main sequence. The evolutionary sequence is somewhat controversial (see below) and may in fact describe the evolutionary phase of the circumstellar material rather than of the star itself.

At first inspection, and especially in the outer reaches of the molecular clouds such as the ρ Oph cloud (André et al. 1987, 1988, Stine et al. 1988, Magazzù et al. 1999), one encounters predominantly WTTS that appear to have evolved past the CTT phase. How early in its infancy can a star be to develop strong radio signatures? Whereas deeper surveys of ρ Oph have accessed several deeply embedded infrared sources with high radio luminosities ($\log L_R > 15$, some of which are class I sources, André et al. 1987, Brown 1987, Leous et al. 1991, Feigelson et al. 1998) many of the radio-strong WTTS in the ρ Oph dark cloud are significantly closer to the sites of current star formation, and therefore younger, than the typical radio-weaker WTTS and CTTS. It seems that radio-strong WTTS evolve directly from embedded protostars. André et al. (1992) speculated that in some cases strong fossil magnetic fields accelerate both dissipation of circumstellar material and formation of large magnetospheric structures on short time scales

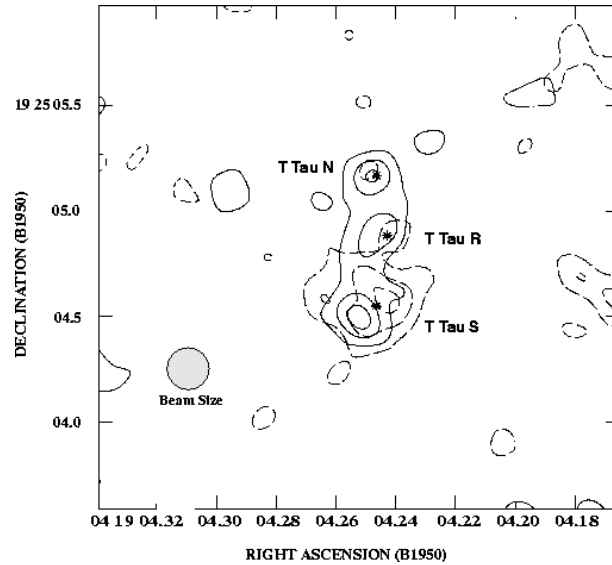


Figure 11: Observation of the T Tau system at 6 cm with the MERLIN interferometer. Right- and left-hand circularly polarized components are shown dashed and solid, respectively. The offset of the polarized flux centroids in T Tau(S) is interpreted in terms of polarized outflows (Ray et al. 1997; reproduced with the permission of Nature.)

of $\sim 10^6$ years.

Genuine, embedded class I protostars have most often been detected as thermal sources, and this emission is predominantly due to collimated thermal winds or jets. These jets are probably ionized by neutral winds that collide with the ambient medium at distances of around 10 AU and that are aligned with molecular outflows (Bieging & Cohen 1985, Snell et al. 1985, Brown 1987, Curiel et al. 1987, 1989, 1990, Rodríguez et al. 1989, 1990, 1995, Morgan et al. 1990, Martí et al. 1993, Garay et al. 1996, Suturs et al. 1996, Torrelles et al. 1997). In the case of more massive stars, the radio emission can also originate from optically thick or thin compact HII regions (e.g., Hughes 1988, Estalella et al. 1991, Gómez et al. 2000), or from ionized winds (Felli et al. 1998); even (thermal or non-thermal) gyrosynchrotron emission has been proposed given the high brightness temperatures, small sizes, variability, and negative spectral indices of some sources (Hughes 1991, Hughes et al. 1995, Garay et al. 1996). For a review of thermal radio jets driving outflows and Herbig-Haro objects, see, e.g., Anglada (1995, 1996), and Anglada et al. (1998). Ionized circumstellar material and winds easily become optically thick and therefore occult any non-thermal, magnetic emission from close to the star. However, the discovery of polarization in T Tau(S) (Phillips et al. 1993), in IRS 5 (Feigelson et al. 1998), in protostellar jet sources (Yusef-Zadeh et al. 1990) and the jet outflows themselves (Curiel et al. 1993, Hughes 1997, Ray et al. 1997; Figure 11), as well as variability and negative spectral indices in T Tau(S) (Skinner & Brown 1994) provided definitive evidence for magnetic fields and particle acceleration in these class I objects.

Moving toward the youngest accreting or class 0 sources, centimetric thermal radio detections probably again relate to jets/collimated winds that drive massive outflows, whereas the bulk of the emitted power leaves the system at mm/submm wavelengths from cold ($\lesssim 20$ K) dust, a defining property of class 0 protostars (André et al. 1993). Several objects have been detected, with ages of the order of only 10^4 years and central stellar masses of only $\approx 0.05M_{\odot}$ (Leous et

al. 1991, André et al. 1993, Bontemps et al. 1995, Yun et al. 1996, André et al. 1999, Gibb 1999, Reipurth et al. 1999), marking the very beginning of the protostellar accretion phase. Radio emission is thus a sensitive tracer for the presence of an embedded, nascent but already formed protostellar core as opposed to a contracting cloud fragment (see, e.g., Yun et al. 1996).

11.2 Evolution to the Main Sequence

Early VLA surveys of CTTS quickly recognized their thermal wind-type emission with rising spectra and large angular sizes (Cohen et al. 1982, Bieging et al. 1984, Cohen & Bieging 1986, Schwartz et al. 1984, 1986). The enormous kinetic wind energy derived under the assumption of a uniform spherical wind suggests anisotropic outflows while structural changes in the radio sources indicate variable outflows, probably along jet-like features (Cohen & Bieging 1986). Mass loss rates are estimated to be $\lesssim 10^{-7} M_{\odot} \text{ yr}^{-1}$ (André et al. 1987). It is important to note that the thermal radio emission says nothing about the presence or absence of stellar magnetic fields. CTTS do show a number of magnetically induced phenomena, but whatever the possible accompanying radio emission, it is thought to be absorbed by the circumstellar ionized wind, unless huge magnetospheric structures reach beyond the optically thick wind surface (Stine et al. 1988, André et al. 1992).

The CTT stage is pivotal for planetary system formation as massive accretion disks are present. Their dust emission dominates the systemic luminosity at millimeter wavelengths. Large (>1000 AU) molecular and dust features have been mapped at such wavelengths; however, observations of the solar-system sized inner disks (100 AU) have been challenging and require high angular resolution. At cm wavelengths, thermal collimated outflows may become dominant over dust disks but both features can be mapped simultaneously in some cases, revealing two orthogonal structures, one a jet and one an edge-on disk (Rodríguez et al. 1992, 1994, Wilner et al. 1996).

At ages of typically $1 - 20 \times 10^6$ years, most T Tau stars dissipate their accretion disks and circumstellar material and become similar to main-sequence stars albeit at much higher magnetic activity levels, probably induced by their short rotation periods (O’Neal et al. 1990, White et al. 1992a). The presence of huge flares (Feigelson & Montmerle 1985, Stine et al. 1988, Stine & O’Neal 1998), longer-term variability, and falling spectra clearly point to non-thermal gyrosynchrotron emission (Bieging et al. 1984, Kutner et al. 1986, Bieging & Cohen 1989, White et al. 1992a, Felli et al. 1993, Phillips et al. 1996) analogous to more evolved active stars. Conclusive radio evidence for the presence of solar-like magnetic fields in WTTS came with the detection of weak circular polarization during flare-like modulations, but also in quiescence (White et al. 1992b, André et al. 1992, Skinner 1993). Zeeman measurements confirm the presence of kGauss magnetic fields on the surface of some of these stars (e.g., Johns-Krull et al. 1999). Extreme particle energies radiating synchrotron emission may be involved, giving rise to linear polarization in flares on the WTT star HD 283447 (Phillips et al. 1996). VLBI observations showing large ($\sim 10R_*$) magnetospheric structures with brightness temperatures of $T_b \approx 10^9$ K fully support the non-thermal picture (Phillips et al. 1991).

As a WTT star ages, its radio emission drops rapidly on time scales of a few Million years from luminosities as high as $10^{18} \text{ erg s}^{-1} \text{ Hz}^{-1}$ to values around or below $10^{15} \text{ erg s}^{-1} \text{ Hz}^{-1}$ at ages beyond 10 Myr. Young age of a star is thus favorable for strong radio emission (O’Neal et al. 1990, White et al. 1992a, Chiang et al. 1996), whereas toward the subsequent Zero-Age Main-Sequence (ZAMS) stage it is only the very rapid rotators that keep producing radio emission at a $10^{15} \text{ erg s}^{-1} \text{ Hz}^{-1}$ level (Carkner et al. 1997, Magazzù et al. 1999, Mamajek et al. 1999).

11.3 Low-Mass Stars on the Main Sequence

The pace at which radio emission decays toward the ZAMS has prevented systematic radio detections of cool main-sequence stars beyond 10–20 pc. Much of the evolutionary trends known to date have been derived from fairly small and very select samples of extraordinary stars. Although many nearby M dwarfs are probably quite young and located near the ZAMS, their ages are often not well known. An interesting exception is the proper-motion dM4e companion to AB Dor, Rst137B, detected as a surprisingly luminous steady and flaring radio star (Lim 1993, Beasley & Cram 1993). With an age of $\sim 5 - 8 \times 10^7$ years, it may indicate that stars approaching the main sequence go through a regime of strongly enhanced magnetic activity. The AB Dor pair is a member of the Local Association, also known as the Pleiades Moving Group, a star stream of an age (~ 50 –100 Million years) corresponding to near-ZAMS for F–K stars. A handful of further stream members with vigorous radio emission are now known in the solar neighborhood, most notably PZ Tel (cited in Lim & White 1995), HD 197890 (K1 V; Robinson et al. 1994), HD 82558 (K1 V, Drake et al. 1990), EK Dra (G0 V, Güdel et al. 1994, 1995a), and 47 Cas (F0 V + G V; Güdel et al. 1995c, 1998).

These objects are analogs of young open cluster stars with the observational advantage of being much closer. Clusters, however, are preferred when more precise stellar ages or large statistics are required. Some young clusters house a select group of ultra-fast rotators, stars at the extreme of dynamo operation with rotation periods $\lesssim 1$ day. The absence of any detections in Bastian et al.’s (1988) Pleiades radio survey suggests that their flare properties are similar to solar neighborhood stars rather than to the much more energetic outbursts occasionally seen in star forming regions. Flaring or quiescent radio emissions have been detected from G–K-type members of both the Pleiades (Lim & White 1995) and the Hyades (White et al. 1993, Güdel et al. 1996b) although these examples, in part ultra-fast rotators at saturated activity levels and in part binary systems, clearly represent only the extreme upper end of magnetic activity. Radio emission of normal, single solar analogs rapidly declines to undetectable levels after a few hundred Million years (Gaidos et al. 2000).

11.4 Herbig Ae/Be stars

The evolution of intermediate-mass ($3 - 20 M_{\odot}$) stars is quite different from, and much faster than, that of low-mass stars as they still accrete while already on the main sequence. Given their intermediate spectral range, it is of great interest to know whether Herbig Ae/Be pre-main sequence stars support convective, magnetic dynamos or whether they resemble more massive wind sources. Radio emission is the ideal discriminator. A wind-mass loss interpretation is compatible with the expected mass loss rates of $10^{-6} - 10^{-8} M_{\odot} \text{yr}^{-1}$ (Güdel et al. 1989b, Skinner et al. 1993). This interpretation is supported by the large radio sizes (order of $1''$) and the absence of circular polarization or strong variability. The radio luminosity is also correlated with the stellar temperature and bolometric luminosity. This is expected because wind mass-loss rates increase toward higher stellar masses (Skinner et al. 1993). New radio observations complemented by millimeter measurements further indicate the presence of substantial dust envelopes (Di Francesco et al. 1997).

Non-thermal gyrosynchrotron sources exist as well among Herbig stars, although they are the exception (Skinner et al. 1993). The evidence comes primarily from negative spectral indices, including the extremely X-ray strong proto-Herbig star EC95 = S68-2 that further supports a coronal model based on its L_X/L_R ratio (Smith et al. 1999).

12 STARS AT THE INTERFACE BETWEEN HOT WINDS AND CORONAE

Owing to missing convection, no dynamo-generated magnetic fields are expected on stars earlier than spectral type F, nor should there be massive ionized winds on main-sequence stars of spectral type B and later, given the weak radiation pressure. Indeed, few detections have been reported as early as spectral type F0, although some have been found at quite high luminosities compatible with the gyrosynchrotron mechanism, including main-sequence candidates (Güdel et al. 1995b) and the supergiant α Car (Slee & Budding 1995). Brown et al. (1990) surveyed a number of normal A-type stars and found stringent upper limits to any radio emission and thus to the mass-loss rate - very much in agreement with expectations. However, as it turns out, this spectral range is shared by some of the more provocative radio detections.

Many “magnetic chemically peculiar” Bp/Ap stars maintain considerable radio emission ($\log L_R \approx 15 - 18$; Drake et al. 1987b), including very young objects such as S1 in ρ Oph (André et al. 1988). They all relate to the hotter (O9–A0 spectral type) He-strong and He-weak/Si-strong classes, whereas the cooler (A type) SrCrEu peculiarity classes remain undetected (Drake et al. 1987b, Willson et al. 1988, Linsky et al. 1992, Leone et al. 1994). Similarly, “non-magnetic” Am and HgMn stars remain undetected despite recent claims that these stars may have magnetic fields as well (Drake et al. 1994). The emission mechanism is likely to be gyrosynchrotron as judged from flat spectra (Linsky et al. 1992, Leone et al. 1996), high brightness temperature (Phillips & Lestrade 1988), variability, and sometimes moderate polarization (Linsky et al. 1992).

The presence of kilogauss magnetic fields on magnetic chemically peculiar stars has been known since 1947 (Babcock 1947). The fields are generally assumed to be of global, dipolar topology. There is little photospheric motion that could stir magnetic footpoints, but weak winds could draw the magnetic field lines into an equatorial current sheet, thus producing a global “van Allen Belt” magnetospheric structure as described in “Magnetospheric Models,” above. Estimated non-thermal source radii are a few stellar radii, confirmed by VLBI observations (Phillips & Lestrade 1988, André et al. 1991) that also conclusively established the non-thermal nature of the radio emission, with brightness temperatures of $T_b \approx 10^8 - 10^9$ K.

The wind-controlled magnetospheric model is further supported qualitatively by a parameter dependence of the form $L_R \propto \dot{M}^{0.38} B_{\text{rms}}^{1.06} P_{\text{rot}}^{-0.32}$ where \dot{M} is the estimated wind mass-loss rate for the spectral type, B_{rms} is the root-mean square value of the longitudinal magnetic field, and P_{rot} is the stellar rotation period (the dependence on the latter is marginal; Linsky et al. 1992). Evidence for rotational modulation probably due to field misalignment has been found by Leone (1991), Leone & Umana (1993), and Lim et al. (1996b), the latter authors reporting modulation of the polarization degree and sign. A surprise detection was the phase-dependent 100% polarized radio emission from a Bp star that suggests a strongly beamed, continuously radiating electron cyclotron maser (Trigilio et al. 2000).

A binary class in this spectral range that is thought to be intermediate in evolution between the young semi-detached B-type β Lyr system that shows radio evidence for large systemic wind mass loss (Umana et al. 2000), and evolved normal Algol binaries with non-thermal coronal emission is defined by the rather inhomogeneous sample of Serpentid stars or “Peculiar Emission Line Algols” (PELAs). These typically consist of an A–B type primary and a F–K type companion with strong mass transfer into a geometrically thick accretion disk around the early-type star, and a common, thin envelope. They have shown an appreciable level of radio emission, first thought to be gyrosynchrotron emission based on their large luminosities (Elias 1990) but later suspected to be wind sources given their spectral indices close to the standard wind law (Elias & Güdel 1993).

13 RADIO EMISSION FROM BROWN DWARFS

Brown dwarf stars have masses below the critical mass of $\approx 0.08M_{\odot}$ required for stable hydrogen burning in the stellar core. Detecting radio emission that shows variability, polarization, or gyrosynchrotron-like spectra from brown dwarfs would provide very strong evidence for the existence of surface magnetic fields. However, after brown dwarfs cease to burn deuterium, the internal convection decreases, probably diminishing the generation of magnetic fields (Neuhäuser et al. 1999). A deep 3.6 cm survey with the VLA, concentrating on older targets, did indeed fail to produce radio detections (Krishnamurthi et al. 1999). One young candidate brown dwarf has been reported with strongly variable radio emission (P. André, cited in Wilking et al. 1999 and Neuhäuser et al. 1999). But again, nature offered more riddles: The first radio-detected bona-fide brown dwarf, LP944-20, is in fact quite old (~ 500 Million years), but showed both flaring and quiescent episodes (Berger et al. 2001). Its radio emission is orders of magnitude higher than would be expected from the active-stellar relation (28). In any case, the observed flaring radio emission is a telltale signature of magnetic fields, and proves that solar-like coronal activity is present in substellar objects - even old ones.

A promising method for detecting sub-stellar objects with sufficiently strong magnetic fields involves the operation of the cyclotron maser. In fact, Jupiter's decametric radiation can be as strong as solar coherent bursts, although at somewhat longer wavelengths. Searching nearby stars for low-frequency coherent bursts may, by positional analysis, reveal companion planets or brown dwarfs. Such a study was performed by Winglee et al. (1986), albeit with null results. We note in passing that one of their targets, Gl 411/Lalande 21185, has in the meantime been shown by astrometric means to possess at least one planetary companion (Gatewood 1996).

14 STELLAR ASTROMETRY

VLBI techniques have been used for astrometric purposes, i.e., measurements of positions, proper motions, binary orbital motions, and parallaxes, to an accuracy of fractions of a milliarcsecond (Lestrade et al. 1990, 1993, 1995, 1999). While one fundamental purpose of such programs is to establish the astrometric link between the radio and the optical coordinate reference frames that is eventually of great importance for numerous dynamical studies, invaluable astrophysical spin-offs were obtained. Astrometry of the Algol triple system (a 2.9-day period A7m+K0 IV close binary with mass exchange, in a wide 680 d orbit around a B8 V star) showed unequivocally that the radio emission is related to the magnetically active K subgiant. The most startling result (confirming earlier, indirect optical polarization measurements) was that the planes of the short and the long orbits are orthogonal to each other (Lestrade et al. 1993, 1999), a challenge for stability theories. Further important highlights include i) precise measurements of distances through parallaxes, including distances to star forming regions, ii) identification of binarity or multiple systems, and iii) rapidly moving ejecta after a stellar flare (see Lestrade et al. 1999 for details). A dedicated pre-Hipparcos VLBI study of the AB Doradus system solved for the accurate distance (moving the star to 2/3 its previously assumed distance and placing it on the ZAMS) and for a short-period disturbance attributed to the presence of a low-mass object (possibly a brown dwarf) in orbit around this star (Guirado et al. 1997).

15 SUMMARY AND CONCLUSIONS

Stellar radio astronomy has matured over the past few decades to a science that is indispensable for our understanding of stellar atmospheres. Historical milestones include, among many others,

the discovery of steady and flaring non-thermal and polarized emission in cool stars, testifying to the importance of highly energetic processes; the recognition that these phenomena are ubiquitous in many classes of convective-envelope stars; observations of very large, apparently stable magnetospheric structures, unlike anything known from the Sun, around various types of magnetically active stars such as T Tau stars, Bp stars, dMe stars, or RS CVn binaries; the discovery of non-thermal emission produced in (wind-collision) shocks of hot-star atmospheres; gyromagnetic and flaring emission from deeply embedded protostellar objects, testifying to the importance of magnetic fields back to the earliest moments of a stellar life; and flaring radio emission from sub-stellar objects not previously thought to support stellar-like convective outer envelopes. Radio methodology has become a standard to estimate magnetic fields in cool stars, to determine mass loss in stars with ionized winds, to spatially resolve and map structures at the milliarcsecond level, and to simply prove the presence of magnetic fields through polarization measurements.

Far from being an auxiliary science to research at other wavelengths, stellar radio astronomy should prepare to address outstanding problems to which it has unique access, although more sensitive instruments are needed. Questions of particular interest include: Are there relevant high-energy processes and magnetic fields in class 0 protostars? Are accretion processes important for the high-energy mechanisms and the generation of large-scale magnetic fields? Are there magnetic fields in hot stars, and what role do they play in the winds? Are brown dwarfs usually quiescent radio emitters? Do they maintain stable magnetic fields? What is the structure of their coronae? Are there intra-binary magnetic fields in close binary stars? How do large magnetospheres couple to the more compact X-ray coronae? Are quiescent coronae fed by numerous (micro-)flares?

Acknowledgements: It is a pleasure to thank Marc Audard, Arnold Benz, Stephen Skinner, Kester Smith, and Stephen White for helpful discussions, and Philippe André, Tim Bastian, Arnold Benz, Maria Contreras, Jeremy Lim, Robert Mutel, Tom Ray, Luis Rodríguez, and Stephen White for providing figure material. The introductory Einstein quotation is cited from "Einstein sagt", ed A Calaprice and A Ehlers (1997, Munich: Piper) and from "The Expanded Quotable Einstein", ed A Calaprice (2000, Princeton: Princeton University Press).

Literature Cited

- Abada-Simon M, Lecacheux A, Aubier M, Bookbinder JA. 1997. *Astron. Astrophys.* 321:841–49
 Abada-Simon M, Lecacheux A, Louarn P, Dulk GA, Belkora L, et al. 1994. *Astron. Astrophys.* 288:219–30
 Abbott DC, Bieging JH, Churchwell E. 1984. *Ap. J.* 280:671–78
 Abbott DC, Bieging JH, Churchwell E, Torres AV. 1986. *Ap. J.* 303:239–61
 Airapetian VS, Holman GD. 1998. *Ap. J.* 501:805–12
 Alef W, Benz AO, Güdel M. 1997. *Astron. Astrophys.* 317:707–11
 André P. 1996. In *Radio Emission from the Stars and the Sun*, ed. AR Taylor, JM Paredes, ASP Conf. Ser. 93, pp. 273–84. San Francisco: ASP
 André P, Deeney BD, Phillips RB, Lestrade J-F. 1992. *Ap. J.* 401:667–77
 André P, Montmerle T, Feigelson ED. 1987. *Astron. J.* 93:1182–98
 André P, Montmerle T, Feigelson ED, Stine PC, Klein K-L. 1988. *Ap. J.* 335:940–52
 André P, Motte F, Bacmann A. 1999. *Ap. J. Lett.* 513:L57–60
 André P, Phillips RB, Lestrade J-F, Klein K-L. 1991. *Ap. J.* 376:630–35
 André P, Ward-Thompson D, Barsony M. 1993. *Ap. J.* 406:122–41
 Anglada G. 1995. *Rev. Mex. Astron. Astrofis.* 1:67–76
 Anglada G. 1996. See André 1996, pp. 3–14
 Anglada G, Villuendas E, Estalella R, Beltrán MT, Rodríguez LF, et al. 1998. *Astron. J.* 116:2953–64
 Aschwanden MJ. 1987. *Sol. Phys.* 111:113–36

- Ayres TR, Brown A, Osten RA, Huenemoerder DP, Drake, JJ, et al. 2001. *Ap. J.* 549:554–77
- Babcock HW. 1947. *Ap. J.* 105:105–19
- Baliunas SL, Donahue RA, Soon W, Henry GW. 1998. In *10th Cambridge Workshop on Cool Stars, Stellar Systems, and the Sun*, ed. R. Donahue, JA Bookbinder, pp. 153–72. San Francisco: ASP
- Bastian TS. 1990. *Sol. Phys.* 130:265–94
- Bastian TS. 1996. See André 1996, pp. 447–54
- Bastian TS, Benz AO, Gary DE. 1998. *Annu. Rev. Astron. Astrophys.* 36:131–88
- Bastian TS, Bookbinder JA. 1987. *Nature* 326:678–80
- Bastian TS, Bookbinder J, Dulk GA, Davis M. 1990. *Ap. J.* 353:265–73
- Bastian TS, Dulk GA, Slee OB. 1988. *Astron. J.* 95:794–803
- Beasley AJ, Ball LT, Budding E, Slee OB, Stewart RT. 1993. *Astron. J.* 106:1656–59
- Beasley AJ, Cram LE. 1993. *MNRAS* 264:570–78
- Beasley AJ, Güdel M. 2000. *Ap. J.* 529:961–67
- Becker RH, White RL. 1985. *Ap. J.* 297:649–51
- Bell AR. 1978. *MNRAS* 182:147–56
- Benz AO. 2002. *Plasma Astrophysics*. Dordrecht:Kluwer
- Benz AO, Alef W. 1991. *Astron. Astrophys. Lett.* 252:L19–22
- Benz AO, Alef W, Güdel M. 1995. *Astron. Astrophys.* 298:187–92
- Benz AO, Conway J, Güdel M. 1998. *Astron. Astrophys.* 331:596–600
- Benz AO, Güdel M. 1994. *Astron. Astrophys.* 285:621–30
- Benz AO, Magun A, Stehling W, Hai S. 1992. *Sol. Phys.* 141:335–46
- Berger E, Ball S, Becker KM, Clarke M, Frail DA, et al. 2001. *Nature* 410:338–40
- Bieging JH, Abbott DC, Churchwell EB. 1982. *Ap. J.* 263:207–14
- Bieging JH, Abbott DC, Churchwell EB. 1989. *Ap. J.* 340:518–36
- Bieging JH, Cohen M. 1985. *Ap. J. Lett.* 289:L5–8
- Bieging JH, Cohen M. 1989. *Astron. J.* 98:1686–92
- Bieging JH, Cohen M, Schwartz PR. 1984. *Ap. J.* 282:699–708
- Bontemps S, André P, Ward-Thompson D. 1995. *Astron. Astrophys.* 297:98–102
- Bookbinder JA. 1988. In *Activity in Cool Stars Envelopes*, ed. O Havnes, BR Pettersen, JHMM Schmitt, JE Solheim, pp. 257–67. Dordrecht: Kluwer
- Bookbinder JA. 1991. *Mem. Soc. Astron. Ital.* 62:321–36
- Borghi S, Chiuderi Drago F. 1985. *Astron. Astrophys.* 143:226–30
- Brown A. 1987. *Ap. J. Lett.* 322:L31–34
- Brown A, Osten RA, Drake SA, Jones KL, Stern RA. 1998. In *The Hot Universe*, ed. K Koyama, S Kitamoto, M Itoh, IAU Symp 188, pp. 215–16. Dordrecht: Kluwer
- Brown A, Vealé A, Judge P, Bookbinder JA, Hubeny I. 1990. *Ap. J.* 361:220–24
- Brown RL, Crane PC. 1978. *Astron. J.* 83:1504–09
- Budding E, Jones KL, Slee OB, Watson L. 1999. *MNRAS* 305:966–76
- Buntun JD, Large MI, Slee OB, Stewart RT, Robinson RD, Thatcher JD. 1989. *Proc. Astron. Soc. Australia* 8:127–31
- Caillault J-P, Chanan GA, Helfand DJ, Patterson J, Nousek JA, et al. 1985. *Nature* 313:376–78
- Caillault J-P, Drake S, Florkowski D. 1988. *Astron. J.* 95:887–93
- Carkner L, Mamajek E, Feigelson E, Neuhäuser R, Wichmann R, Krautter J. 1997. *Ap. J.* 490:735–43
- Chapman JM, Leitherer C, Koribalski B, Bouter R, Storey M. 1999. *Ap. J.* 518:890–900
- Chiang E, Phillips RB, Lonsdale CJ. 1996. *Astron. J.* 111:355–64
- Chiuderi Drago F, Franciosini E. 1993. *Ap. J.* 410:301–8
- Churchwell E, Bieging JH, van der Hucht KA, Williams PM, Spoelstra TATH, Abbott DC. 1992. *Ap. J.* 393:329–40
- Cohen M, Bieging JH. 1986. *Astron. J.* 92:1396–1402
- Cohen M, Bieging JH, Schwartz PR. 1982. *Ap. J.* 253:707–15
- Contreras ME, Rodríguez LF. 1999. *Ap. J.* 512:762–66
- Contreras ME, Rodríguez LF, Gómez Y, Velázquez A. 1996. *Ap. J.* 469:329–35
- Contreras ME, Rodríguez LF, Tapia M, Cardini D, et al. 1997. *Ap. J. Lett.* 488:L153–6
- Cox JJ, Gibson DM. 1985. In *Radio Stars*, ed. RM Hjellming, DM Gibson, pp. 233–36. Dordrecht: Reidel
- Curiel S, Cantó J, Rodríguez LF. 1987. *Rev. Mex. Astron. Astrofis.* 14:595–602
- Curiel S, Raymond JC, Rodríguez LF, Cantó J, Moran JM. 1990. *Ap. J.* 365:L85–88
- Curiel S, Rodríguez LF, Bohigas J, Roth M, Cantó J. 1989. *Astrophys. Lett. Comm.* 27:299–309

- Curiel S, Rodríguez LF, Moran JM, Cantó J. 1993. *Ap. J.* 415:191–203
- Dempsey RC, Neff JE, Lim J. 2001. *Ap. J.* 122:332–348
- Dennis BR, Zarro DM. 1993. *Sol. Phys.* 146:177–90
- Di Francesco J, Evans NJ II, Harvey PM, Mundy LG, Guilloteau S, Chandler CJ. 1997. *Ap. J.* 482:433–41
- Doiron DJ, Mutel RL. 1984. *Astron. J.* 89:430–32
- Dougherty SM, Taylor AR, Waters LBFM. 1991. *Astron. Astrophys.* 248:175–8
- Dougherty SM, Williams PM. 2000. *MNRAS* 319:1005–10
- Dougherty SM, Williams PM, Pollacco DL. 2000. *MNRAS* 316:143–51
- Dougherty SM, Williams PM, van der Hucht KA, Bode MF, Davis RJ. 1996. *MNRAS* 280:963–70
- Doyle JG, Mathioudakis M. 1991. *Astron. Astrophys. Lett.* 241:L41–L42
- Drake SA. 1990. *Astron. J.* 100:572–578
- Drake SA, Abbott DC, Bastian TS, Biegging JH, Churchwell E, et al. 1987b. *Ap. J.* 322:902–8
- Drake SA, Johnson HR, Brown A. 1991b. *Astron. J.* 101:1483–88
- Drake SA, Linsky JL. 1986. *Astron. J.* 91:602–20
- Drake SA, Linsky JL. 1989. *Astron. J.* 98:1831–1841
- Drake SA, Linsky JL, Bookbinder JA. 1994. *Astron. J.* 108:2203–6
- Drake SA, Linsky JL, Elitzur M. 1987a. *Astron. J.* 94:1280–90
- Drake SA, Linsky JL, Judge PG, Elitzur M. 1991a. *Astron. J.* 101:230–36
- Drake SA, Simon T, Brown A. 1993. *Ap. J.* 406:247–51
- Drake SA, Simon T, Linsky JL. 1986. *Astron. J.* 91:1229–32
- Drake SA, Simon T, Linsky JL. 1987c. *Astron. J.* 92:163–167
- Drake SA, Simon T, Linsky JL. 1989. *Ap. J. Suppl.* 71:905–30
- Drake SA, Simon T, Linsky JL. 1992. *Ap. J. Suppl.* 82:311–21
- Drake SA, Walter FM, Florkowski DR. 1990. In *6th Cambridge Workshop on Cool Stars, Stellar Systems, and the Sun*, ed. G Wallerstein, pp. 148–51. San Francisco: ASP
- Dulk GA. 1985. *Annu. Rev. Astron. Astrophys.* 23:169–224
- Dulk GA. 1987. In *5th Cambridge Workshop on Cool Stars, Stellar Systems, and the Sun*, ed. JL Linsky, RE Stencel, pp. 72–82. Berlin: Springer
- Dulk GA, Marsh KA. 1982. *Ap. J.* 259:350–58
- Eichler D, Usov V. 1993. *Ap. J.* 402:271–79
- Elias, NM II. 1990. *Ap. J.* 352:300–2
- Elias NM II, Güdel M. 1993. *Astron. J.* 106:337–41
- Elias NM II, Quirrenbach A, Witzel A, Naundorf CE, Wegner R, et al. 1995. *Ap. J.* 439:983–90
- Estalella R, Anglada G, Rodríguez LF, Garay G. 1991. *Ap. J.* 371:626–30
- Feigelson ED, Carkner L, Wilking BA. 1998. *Ap. J. Lett.* 494:L215–18
- Feigelson ED, Montmerle T. 1985. *Ap. J. Lett.* 289:L19–23
- Feldman PA, Taylor AR, Gregory PC, Seaquist ER, Balonek TJ, Cohen NL. 1978. *Astron. J.* 83:1471–84
- Felli M, Massi M. 1991. *Astron. Astrophys.* 246:503–6
- Felli M, Massi M., Catarzi M. 1991. *Astron. Astrophys.* 248:453–57
- Felli M, Massi M, Churchwell E. 1989. *Astron. Astrophys.* 217:179–86
- Felli M, Taylor GB, Catarzi M, Churchwell E, Kurtz S. 1993. *Astron. Astrophys. Suppl.* 101:127–51
- Felli M, Taylor GB, Neckel Th, Staude HJ. 1998. *Astron. Astrophys.* 329:243–48
- Fox DC, Linsky JL, Vealé A, Dempsey RC, Brown A, et al. 1994. *Astron. Astrophys.* 284:91–104
- Franciosini E, Chiuderi Drago F. 1995. *Astron. Astrophys.* 297:535–42
- Franciosini E, Massi M, Paredes JM, Estalella R. 1999. *Astron. Astrophys.* 341:595–601
- Gaidos E, Güdel M, Blake GA. 2000. *Geophys. Res. Lett.* 27:501–3
- Garay G, Moran JM, Reid MJ. 1987. *Ap. J.* 314:535–50
- Garay G, Ramírez S, Rodríguez LF, Curiel S, Torrelles JM. 1996. *Ap. J.* 459:193–208
- Gary DE, Linsky JL. 1981. *Ap. J.* 250:284–92
- Gary DE, Linsky JL, & Dulk GA. 1982. *Ap. J. Lett.* 263:L79–83
- Gatewood G. 1996. *Bull. Am. Astron. Soc.* 188:40.11 (Abstr)
- Gibb AG. 1999. *MNRAS* 304:1–7
- Gibson DM. 1983. In *3rd Cambridge Workshop on Cool Stars, Stellar Systems, and the Sun*, ed. SL Baliunas, L Hartmann, pp. 197–201. Berlin: Springer Verlag
- Gómez Y, Rodríguez LF, Garay G. 2000. *Ap. J.* 531:861–7
- Güdel M. 1994. *Ap. J. Suppl.* 90:743–51

- Güdel M, Audard M, Smith K, Behar E, Beasley AJ, Mewe R. 2002. *Ap. J.*, in press
- Güdel M, Benz AO. 1989. *Astron. Astrophys. Lett.* 211:L5–8
- Güdel M, Benz AO. 1993. *Ap. J. Lett.* 405:L63–L66
- Güdel M, Benz AO, Bastian TS, Fürst E, Simnett GM, Davis RJ. 1989a. *Astron. Astrophys. Lett.* 220:L5–L8
- Güdel M, Benz AO, Catala C, Praderie F. 1989b. *Astron. Astrophys. Lett.* 217:L9–12
- Güdel M, Benz AO, Guinan EF, Schmitt JHMM. 1996b. See André 1996, pp. 306–8
- Güdel M, Benz AO, Schmitt JHMM, Skinner SL. 1996a. *Ap. J.* 471:1002–14
- Güdel M, Guinan EF, Etzel PB, Mewe R, Kaastra JS, Skinner SL. 1998. See Baliunas et al. 1998, pp. 1247–56
- Güdel M, Schmitt JHMM, Benz AO. 1994. *Science* 265:933–35
- Güdel M, Schmitt JHMM, Benz AO. 1995b. *Astron. Astrophys.* 302:775–87
- Güdel M, Schmitt JHMM, Benz AO. 1995c. *Astron. Astrophys. Lett.* 293:L49–L52
- Güdel M, Schmitt JHMM, Benz AO, Elias NM II. 1995a. *Astron. Astrophys.* 301:201–12
- Güdel M, Schmitt JHMM, Bookbinder JA, Fleming TA. 1993. *Ap. J.* 415:236–39
- Guirado JC, Reynolds JE, Lestrade J-F, Preston RA, Jauncey DL, et al. 1997, *Ap. J.* 490:835–39
- Gunn AG, Brady, PA, Migenes V, Spencer RE, Doyle JG. 1999. *MNRAS* 304:611–21
- Gunn AG, Migenes V, Doyle JG, Spencer RE, Mathioudakis M. 1997. *MNRAS* 287:199–210
- Havnes O, Goertz CK. 1984, *Astron. Astrophys.* 138:421–30
- Hawley SL, Fisher GH, Simon T, Cully SL, Deustua SE, et al. 1995. *Ap. J.* 453:464–79
- Helfand DJ, Schnee S, Becker RH, White RL, McMahon RG. 1999. *Astron. J.* 117:1568–77
- Hjellming RM. 1988. In *Galactic and Extragalactic Radio Astronomy*, ed. Verschur GL, Kellermann KI, p. 381–438. Berlin: Springer-Verlag
- Hjellming RM, Gibson DM, eds. 1985. *Radio Stars*. Dordrecht: Reidel. 411 pp.
- Holman GD. 1985. *Ap. J.* 293:584–94
- Holman GD. 1986. In *4th Cambridge Workshop on Cool Stars, Stellar Systems, and the Sun*, ed. M Zeilik, DM Gibson, pp. 271–74. Berlin: Springer-Verlag
- Hughes VA. 1988. *Ap. J.* 333:788–800
- Hughes VA. 1991. *Ap. J.* 383:280–88
- Hughes VA. 1997. *Ap. J.* 481:857–65
- Hughes VA, Cohen RJ, Garrington S. 1995. *MNRAS* 272:469–80
- Hughes VA, McLean BJ. 1984. *Ap. J.* 278:716–20
- Hughes VA, McLean BJ. 1987. *Ap. J.* 313:263–7
- Jackson PD, Kundu MR, White SM. 1987. *Ap. J. Lett.* 316:L85–L90
- Jackson PD, Kundu MR, White SM. 1989. *Astron. Astrophys.* 210:284–94
- Johns-Krull CM, Valenti JA, Hatzes AP, Kanaan A. 1999. *Ap. J.* 510:L41–4
- Jones KL, Brown A, Stewart RT, Slee OB. 1996. *MNRAS* 283:1331–39
- Jones KL, Stewart RT, Nelson GJ. 1995. *MNRAS* 274:711–16
- Jones KL, Stewart RT, Nelson GJ, Duncan AR. 1994. *MNRAS* 269:1145–51
- Kellermann KI, Pauliny-Toth IIK. 1969. *Ap. J. Lett.* 155:L71–78.
- Klein K-L. 1987. *Astron. Astrophys.* 183:341–50
- Klein K-L, Chiuderi-Drago F. 1987. *Astron. Astrophys.* 175:179–85
- Knapp GR, Bowers PF, Young K, Phillips TG. 1995. *Ap. J.* 455:293–99
- Krishnamurthi A, Leto G, Linsky JL. 1999. *Astron. J.* 118:1369–72
- Kuijpers J. 1985. See Cox & Gibson 1985, pp. 3–31
- Kuijpers J. 1989a. *Sol. Phys.* 121:163–85
- Kuijpers J. 1989b. In *Plasma phenomena in the solar atmosphere*, ed. MA Dubois, F Bely-Dubau, D. Gresillon D, pp. 17–31. Les Ulis, France: Les Editions de Physique
- Kuijpers J, van der Hulst JM. 1985. *Astron. Astrophys.* 149:343–50
- Kundu MR, Jackson PD, White SM, Melozzi M. 1987. *Ap. J.* 312:822–29
- Kundu MR, Pallavicini R, White SM, Jackson PD. 1988, *Astron. Astrophys.* 195:159–71
- Kundu MR, Shevgaonkar RK. 1985. *Ap. J.* 297:644–48
- Kundu MR, Shevgaonkar RK. 1988. *Ap. J.* 334:1001–7
- Kutner ML, Rydgren AE, Vrba FJ. 1986. *Astron. J.* 92:895–97
- Lang KR. 1990. In *Flare stars in star clusters, associations and the solar vicinity*, ed LV Mirzoyan, BR Pettersen, MK Tsvetkov, IAU Symp. 137, pp. 125–37. Dordrecht: Kluwer
- Lang KR. 1994. *Ap. J. Suppl.* 90:753–64
- Lang KR. 1999. *Astrophysical Formulae*, Vol I. Berlin:Springer Verlag. 614 pp.

- Lang KR, Bookbinder J, Golub L, Davis MM. 1983. *Ap. J. Lett.* 272:L15–18
- Lang KR, Willson RF. 1986a. *Ap. J. Lett.* 302:L17–21
- Lang KR, Willson RF. 1986b. *Ap. J.* 305:363–68
- Lang KR, Willson RF. 1988a. *Ap. J.* 326:300–4
- Lang KR, Willson RF. 1988b. *Ap. J.* 328:610–16
- Large MI, Beasley AJ, Stewart RT, Vaughan AE. 1989. *Proc. Astron. Soc. Australia* 8:123–26
- Lebach DE, Ratner MI, Shapiro II, Ransom RR, Bietenholz MF, et al. 1999. *Ap. J. Lett.* 517:L43–46
- Lefèvre E, Klein K-L, Lestrade J-F. 1994. *Astron. Astrophys.* 283:483–92
- Leitherer C, Chapman JM, Koribalski B. 1995. *Ap. J.* 450:289–301
- Leitherer C, Chapman JM, Koribalski B. 1997. *Ap. J.* 481:898–911
- Leone F. 1991. *Astron. Astrophys.* 252:198–202
- Leone F, Umana G. 1993. *Astron. Astrophys.* 268:667–70
- Leone F, Trigilio C, Umana G. 1994. *Astron. Astrophys.* 283:908–10
- Leone F, Umana G, Trigilio C. 1996. *Astron. Astrophys.* 310:271–76
- Leous JA, Feigelson ED, André P, Montmerle T. 1991. *Ap. J.* 379:683–88
- Lestrade J-F. 1997. In *Stellar Surface Structure*, ed. KG Strassmeier, JL Linsky, pp. 173–80. Dordrecht: Kluwer
- Lestrade J-F, Jones DL, Preston RA, Phillips RB, Titus MA, et al. 1995. *Astron. Astrophys.* 304:182–188
- Lestrade J-F, Mutel RL, Phillips RB, Webber JC, Niell AE, Preston RA. 1984a. *Ap. J. Lett.* 282:L23–L26
- Lestrade J-F, Mutel RL, Preston RA, Phillips RB. 1988. *Ap. J.* 328:232–42
- Lestrade J-F, Mutel RL, Preston RA, Scheid JA, Phillips RB. 1984b. *Ap. J.* 279:184–87
- Lestrade J-F, Phillips RB, Hodges MW, Preston RA. 1993. *Ap. J.* 410:808–14
- Lestrade J-F, Preston RA, Jones DL, Phillips RB, Rogers AEE, et al. 1999. *Astron. Astrophys.* 344:1014–26
- Lestrade J-F, Rogers AEE, Whitney AR, Niell AE, Phillips RB, Preston RA. 1990. *Astron. J.* 99:1663–73
- Leto G, Pagano I, Linsky JL, Rodonò M, Umana G. 2000. *Astron. Astrophys.* 359:1035–41
- Lim J. 1993. *Ap. J. Lett.* 405:L33–L37
- Lim J, Carilli CL, White SM, Beasley AJ, Marson RG. 1998. *Nature* 392:575–77
- Lim J, Drake SA, Linsky JL. 1996b. See André 1996, pp. 324–26
- Lim J, Nelson GJ, Castro C, Kilkenny D, van Wyk F. 1992. *Ap. J. Lett.* 388:L27–30
- Lim J, White SM. 1995. *Ap. J.* 453:207–13
- Lim J, White SM. 1996. *Ap. J. Lett.* 462:L91–94
- Lim J, White SM, Cully SL. 1996c. *Ap. J.* 461:1009–15
- Lim J, White SM, Nelson GJ, Benz AO. 1994. *Ap. J.* 430:332–41
- Lim J, White SM, Slee OB. 1996a. *Ap. J.* 460:976–83
- Linsky JL. 1996. See André 1996, pp. 439–46
- Linsky JL, Drake SA, Bastian TS. 1992. *Ap. J.* 393:341–56
- Linsky JL, Gary DE. 1983. *Ap. J.* 274:776–83
- Luttermoser DG, Brown A. 1992. *Ap. J.* 384:634–39
- Magazzù A, Umana G, Martín EL. 1999. *Astron. Astrophys.* 346:878–82
- Mamajek EE, Lawson WA, Feigelson ED. 1999. *Publ. Astron. Soc. Australia* 16:257–61
- Martí J, Rodríguez LF, Reipurth B. 1993. *Ap. J.* 416:208–17
- Massi M, Chiuderi-Drago F. 1992. *Astron. Astrophys.* 253:403–6
- Massi M, Felli M, Pallavicini R, Tofani G, Palagi F, Catarzi M. 1988. *Astron. Astrophys.* 197:200–4
- Massi M, Neidhöfer J, Torricelli-Ciamponi G, Chiuderi-Drago F. 1998. *Astron. Astrophys.* 332:149–54
- Melrose DB. 1987. See Dulk 1987, pp. 83–94
- Melrose DB. 1989. *Sol. Phys.* 120:369–381
- Melrose DB, Dulk GA. 1982. *Ap. J.* 259:844–58
- Melrose DB, Dulk GA. 1984. *Ap. J.* 282:308–15
- Miralles MP, Rodríguez LF, Tapia M, Roth M, Persi P, et al. 1994. *Astron. Astrophys.* 282:547–53
- Moran JP, Davis RJ, Bode MF, Taylor AR, Spencer RE, et al. 1989. *Nature* 340:449–50
- Morgan JA, Snell RL, Strom KM. 1990. *Ap. J.* 362:274–83
- Morris DH, Mutel RL. 1988. *Astron. J.* 95:204–14
- Morris DH, Mutel RL, Su B. 1990. *Ap. J.* 362:299–307
- Mullan DJ. 1985. See Cox & Gibson 1985, pp. 173–84
- Mullan DJ. 1989. *Sol. Phys.* 121:239–259
- Mullan DJ, Doyle JG, Redman RO, Mathioudakis M. 1992. *Ap. J.* 397:225–31
- Mutel RL. 1996. In *Magnetodynamic phenomena in the solar atmosphere. Prototypes of stellar magnetic activity*,

- ed. Y Uchida, T Kosugi, HS Hudson, Proceedings of the IAU Colloquium 153, pp. 71–80. Dordrecht: Kluwer
- Mutel RL, Doiron DJ, Lestrade J-F, Phillips RB. 1984. *Ap. J.* 278:220–23
- Mutel RL, Lestrade J-F. 1985. *Astron. J.* 90:493–98
- Mutel RL, Lestrade J-F, Preston RA, Phillips RB. 1985. *Ap. J.* 289:262–68
- Mutel RL, Molnar LA, Waltman EB, Ghigo, FD. 1998. *Ap. J.* 507:371–83
- Mutel RL, Morris DH, Doiron DJ, Lestrade J-F. 1987. *Astron. J.* 93:1220–28
- Mutel RL, Weisberg JM. 1978. *Astron. J.* 83:1499–1503
- Neidhöfer J, Massi M, Chiuderi-Drago F. 1993. *Astron. Astrophys. Lett.* 278:L51–53
- Neuhäuser R, Briceño C, Comerón F, Hearty T, Martín EL, et al. 1999. *Astron. Astrophys.* 343:883–93
- Neupert WM. 1968. *Ap. J. Lett.* 153:L59–L64
- Olson FM. 1975. *Astron. Astrophys.* 39:217–23
- O’Neal D, Feigelson ED, Mathieu RD, Myers PC. 1990. *Astron. J.* 100:1610–17
- Osten RA, Brown A, Ayres TR, Linsky JL, Drake SA, et al. 2000. *Ap. J.* 544:953–76
- Pallavicini R, Willson RF, Lang KR. 1985. *Astron. Astrophys.* 149:95–101
- Panagia N, Felli M. 1975. *Astron. Astrophys.* 39:1–5
- Patterson J, Caillault J-P, Skillman DR. 1993. *Publ. Astron. Soc. Pacific* 105:848–52
- Persi P, Tapia M, Rodríguez LF, Ferrari-Toniolo M, Roth M. 1990. *Astron. Astrophys.* 240:93–97
- Pestalozzi MR, Benz AO, Conway JE, Güdel M. 2000. *Astron. Astrophys.* 353:569–74
- Petrosian V. 1985. *Ap. J.* 299:987–93
- Phillips RB. 1991. In *7th Cambridge Workshop on Cool Stars, Stellar Systems, and the Sun*, ed. MS Giampapa, JA Bookbinder, pp. 309–18. San Francisco: ASP
- Phillips RB, Lestrade J-F. 1988. *Nature* 334:329–31
- Phillips RB, Lonsdale CJ, Feigelson ED. 1991. *Ap. J.* 382:261–69
- Phillips RB, Lonsdale CJ, Feigelson ED. 1993. *Ap. J. Lett.* 403:L43–46
- Phillips RB, Lonsdale CJ, Feigelson ED, Deeney BD. 1996. *Astron. J.* 111:918–29
- Phillips RB, Titus MA. 1990. *Ap. J. Lett.* 359:L15–18
- Ray TP, Muxlow TWB, Axon DJ, Brown A, Corcoran D, et al. 1997. *Nature* 385:415–17
- Reid MJ, Menten KM. 1997. *Ap. J.* 476:327–46
- Reipurth B, Rodríguez LF, Chini R. 1999. *Astron. J.* 118:983–89
- Robinson PA, Melrose DB. 1984. *Aust. J. Phys.* 37:675–704
- Robinson RD, Carpenter KG, Slee OB, Nelson GJ, Stewart RT. 1994. *MNRAS* 267:918–26
- Rodríguez LF, Anglada G, Raga A. 1995. *Ap. J. Lett.* 454:L149–52
- Rodríguez LF, Cantó J, Torrelles JM, Gómez JF, Anglada G, Ho PTP. 1994. *Ap. J. Lett.* 427:L103–6
- Rodríguez LF, Cantó J, Torrelles JM, Gómez JF, Ho PTP. 1992. *Ap. J. Lett.* 393:L29–31
- Rodríguez LF, Ho PTP, Torrelles JM, Curiel S, Cantó J. 1990. *Ap. J.* 352:645–53
- Rodríguez LF, Myers PC, Cruz-González I, Tereby S. 1989. *Ap. J.* 347:461–67
- Rucinski SM. 1991. *Astron. J.* 101:2199–206
- Rucinski SM. 1992. *Publ. Astron. Soc. Pacific* 104:1177–86
- Rucinski SM. 1995. *Astron. J.* 109:2690–97
- Rucinski SM, Krogulec M, Seaquist ER. 1993. *Astron. J.* 105:2308–18
- Rucinski SM, Seaquist ER. 1988. *Astron. J.* 95:1837–40
- Saar SH. 1990. In *Solar Photosphere: Structure, Convection, and Magnetic Fields*, ed. JO Stenflo, IAU Symp. 138, pp. 427–41. Dordrecht: Kluwer
- Schwartz PR, Simon T, Campbell R. 1986. *Ap. J.* 303:233–38
- Schwartz PR, Simon T, Zuckerman B, Howell RR. 1984. *Ap. J. Lett.* 280:L23–26
- Scuderi S, Panagia N, Stanghellini C, Trigilio C, Umana G. 1998. *Astron. Astrophys.* 332:251–67
- Seaquist ER. 1993. *Rep. Prog. Physics* 56(9):1145–1208
- Seaquist ER, Krogulec M, Taylor AR. 1993. *Ap. J.* 410:260–74
- Seaquist ER, Taylor AR. 1990. *Ap. J.* 349:313–27
- Seaquist ER, Taylor AR, Button S. 1984. *Ap. J.* 284:202–10
- Setia Gunawan DYA, de Bruyn AG, van der Hucht KA, Williams PM. 2000. *Astron. Astrophys.* 356:676–90
- Shu FH, Adams FC, Lizano, S. 1987. *Annu. Rev. Astron. Astrophys.* 25:23–81
- Simon T, Fekel FC Jr, Gibson DM. 1985. *Ap. J.* 295:153–61
- Skinner CJ, Dougherty SM, Meixner M, Bode MF, Davis RJ, et al. 1997. *MNRAS* 288:295–306
- Skinner SL. 1991. *Ap. J.* 368:272–8
- Skinner SL. 1993. *Ap. J.* 408:660–67

- Skinner SL, Brown A. 1994. *Astron. J.* 107:1461–68
- Skinner SL, Brown A, Stewart RT. 1993. *Ap. J. Suppl.* 87:217–65
- Skinner SL, Itoh M, Nagase F, Zhekov SA. 1999. *Ap. J.* 524:394–405
- Slee OB, Budding E. 1995. *MNRAS* 277:1063–70
- Slee OB, Nelson GJ, Innis JL, Stewart RT, Vaughan A, Wright AE. 1986. *Proc. Astron. Soc. Australia* 6:312–15
- Slee OB, Nelson GJ, Stewart RT, Wright AE, Innis JL, et al. 1987a. *MNRAS* 229:659–77
- Slee OB, Nelson GJ, Stewart RT, Wright AE, Jauncey DL, et al. 1987b. *MNRAS* 227:467–79
- Slee OB, Stewart RT, Nelson GJ, Wright AE, Dulk GA, et al. 1988. *Astro. Lett. Comm.* 27:247–56
- Sligh VI. 1963. *Nature* 199:682
- Smith KW, Güdel M, Benz AO. 1999. *Astron. Astrophys.* 349:475–84
- Snell RL, Bally J, Strom SE, Strom KM. 1985. *Ap. J.* 290:587–95
- Stern RA, Uchida Y, Walter F, Vilhu O, Hannikainen D, et al. 1992. *Ap. J.* 391:760–72
- Stevens IR. 1995. *MNRAS* 277:163–72
- Stewart RT, Innis JL, Slee OB, Nelson GJ, Wright AE. 1988. *Astron. J.* 96:371–77
- Stine PC, Feigelson ED, André P, Montmerle T. 1988. *Astron. J.* 96:1394–1406
- Stine PC, O’Neal D. 1998. *Astron. J.* 116:890–94
- Storey MC, Hewitt RG. 1996. *Publ. Astron. Soc. Australia* 12:174–79
- Suters M, Stewart RT, Brown A, Zealey W. 1996. *Astron. J.* 111:320–26
- Taylor AR, Paredes JM, eds. 1996. *Radio Emission from the Stars and the Sun*. San Francisco: ASP. 466 pp.
- Taylor AR, Seaquist ER. 1984. *Ap. J.* 286:263–8
- Taylor AR, Waters LBFM, Lamers HJGLM, Persi P, Bjorkman KS. 1987. *MNRAS* 228:811–17
- Taylor AR, Waters LBFM, Bjorkman KS, Dougherty SM. 1990. *Astron. Astrophys.* 231:453–8
- Topka K, Marsh KA. 1982. *Ap. J.* 254:641–45
- Torrelles JM, Gómez JF, Rodríguez LF, Ho PTP, Curiel S, Vázquez R. 1997. *ApJ* 489:744–52
- Torricelli-Ciamponi G, Franciosini E, Massi M, Neidhöfer J. 1998. *Astron. Astrophys.* 333:970–76
- Trigilio C, Buemi CS, Umana G, Rodonò M, Leto P, et al. 2001. *Astron. Astrophys.* 373:181–89
- Trigilio C, Leto P, Leone F, Umana G, Buemi C. 2000. *Astron. Astrophys.* 362:281–88
- Trigilio C, Leto P, Umana G. 1998. *Astron. Astrophys.* 330:1060–66
- Trigilio C, Umana G, Migenes V. 1993. *MNRAS* 260:903–7
- Umana G, Catalano S, Rodonò M. 1991. *Astron. Astrophys.* 249:217–22
- Umana G, Leto P, Trigilio C, Hjellming RM, Catalano S. 1999. *Astron. Astrophys.* 342:709–16
- Umana G, Maxted PFL, Trigilio C, Fender RP, Leone F, Yerli SK. 2000. *Astron. Astrophys.* 358:229–32
- Umana G, Trigilio C, Catalano S. 1998. *Astron. Astrophys.* 329:1010–18
- Umana G, Trigilio C, Hjellming RM, Catalano S, Rodonò M. 1993. *Astron. Astrophys.* 267:126–36
- Umana G, Trigilio C, Tumino M, Catalano S, Rodonò M. 1995. *Astron. Astrophys.* 298:143–50
- van den Oord GHJ. 1996. See André 1996, pp. 263–72
- van den Oord GHJ, de Bruyn AG. 1994. *Astron. Astrophys.* 286:181–93
- van den Oord GHJ, Doyle JG. 1997. *Astron. Astrophys.* 319:578–88
- van den Oord GHJ, Doyle JG, Rodonò M, Gary DE, Henry GW, et al. 1996. *Astron. Astrophys.* 310:908–922
- van den Oord GHJ, Kuijpers J, White NE, van der Hulst JM, Culhane JL. 1989. *Astron. Astrophys.* 209:296–304
- Vaughan AE, Large MI. 1986. *MNRAS* 223:399–403
- Vilhu O, Caillault J-P, Heise J. 1988. *Ap. J.* 330:922–27
- Vilhu O, Rucinski SM. 1983. *Astron. Astrophys.* 127:5–14
- Vilhu O, Tsuru T, Collier Cameron A, Budding E, Banks T, et al. 1993. *Astron. Astrophys.* 278:467–77
- Waldron WL, Corcoran MF, Drake SA, Smale AP. 1998. *Ap. J. Suppl.* 118:217–238
- Wendker HJ. 1995. *Astron. Astrophys. Suppl.* 109:177–79
- White RL. 1985. *Ap. J.* 289:698–708
- White RL, Becker RH. 1995. *Ap. J.* 451:352–58
- White SM. 1996. In *9th Cambridge Workshop on Cool Stars, Stellar Systems, and the Sun*, ed. R Pallavicini, AK Dupree, pp. 21–30, San Francisco: ASP
- White SM. 2000. In *Radio Interferometry: The Saga and the Science*, ed. DG Finley, W Miller Goss, NRAO workshop no 27, pp. 86–111. Associated Universities, Inc.
- White SM, Franciosini E. 1995. *Ap. J.* 444:342–49
- White SM, Jackson PD, Kundu MR. 1989a. *Ap. J. Suppl.* 71:895–904
- White SM, Jackson PD, Kundu MR. 1993. *Astron. J.* 105:563–70
- White SM, Kundu MR, Jackson PD. 1986. *Ap. J.* 311:814–18

- White SM, Kundu MR, Jackson PD. 1989b. *Astron. Astrophys.* 225:112–24
- White SM, Kundu MR, Uchida Y, Nitta N. 1990. See Drake et al. 1990, pp. 239–42
- White SM, Lim J, Kundu MR. 1994. *Ap. J.* 422:293–303
- White SM, Pallavicini R, Kundu MR. 1992a. *Astron. Astrophys.* 257:557–66
- White SM, Pallavicini R, Kundu MR. 1992b. *Astron. Astrophys.* 259:149–54
- Wiling BA, Greene TP, Meyer MR. 1999. *Astron. J.* 117:469–82
- Williams PM, Dougherty SM, Davis RJ, van der Hucht KA, Bode MF, Setia Gunawan DYA. 1997. *MNRAS* 289:10–20
- Williams PM, van der Hucht KA, Bouchet P, Spoelstra TATh, Eenens PRJ, et al. 1992. *MNRAS* 258:461–72
- Williams PM, van der Hucht KA, Pollock AMT, Florkowski DR, van der Woerd H, Wamsteker WM. 1990. *MNRAS* 243:662–84
- Williams PM, van der Hucht KA, Spoelstra TATh. 1994. *Astron. Astrophys.* 291:805–10
- Willson RF, Lang KR. 1987. *Ap. J.* 312:278–83
- Willson RF, Lang KR, Foster P. 1988. *Astron. Astrophys.* 199:255–61
- Wilner DJ, Ho PTP, Rodríguez LF. 1996. *Ap. J. Lett.* 470:L117–21
- Winglee RM, Dulk GA, Bastian TS. 1986. *Ap. J. Lett.* 309:L59–62
- Wood BE, Linsky JL, Müller H-R, Zank GP. 2001. *Ap. J.* 547:L49–52
- Wright AE, Barlow MJ. 1975. *MNRAS* 170:41–51
- Yun JL, Moreira MC, Torrelles JM, Afonso JM, Santos NC. 1996. *Astron. J.* 111:841–45
- Yusef-Zadeh F, Cornwell TJ, Reipurth B, Roth M. 1990. *Ap. J. Lett.* 348:L61–64

List of Figures

HR diagram showing 440 radio-detected stars.	3
Gallery of radio dynamic spectra of M dwarf flares. Upper three panels show a flare on AD Leo, recorded with the Arecibo (top), Effelsberg (middle) and Jodrell Bank (bottom) telescopes in different wavelength ranges (see also Güdel et al. 1989a). Bottom three panels show flares on AD Leo (top and middle) and YZ CMi (bottom) observed at Arecibo (after Bastian et al. 1990, reproduced with permission of the AAS).	9
Radio spectra of the RS CVn binary HR 1099 (upper set) and of the dMe dwarf UV Cet (lower set) at different flux levels. The gently bent spectra are indicative of gyrosynchrotron emission, and the high-frequency part of U-shaped spectra for UV Cet has been interpreted as a gyroresonance component (HR 1099 spectra: courtesy of SM White).	11
Light curves of HR 1099 (<i>left</i>) and UX Ari (<i>right</i>) obtained in the two senses of circular polarization. The brighter of the two polarized fluxes varies rapidly and has been interpreted as 100% polarized coherent emission superimposed on a gradually changing gyrosynchrotron component (White & Franciosini 1995; figures from SM White).	13
<i>Left</i> : Neupert effect seen in an M dwarf star, compared with a solar example in the upper panel (Güdel et al. 1996a). <i>Right</i> : Neupert effect seen in an RS CVn binary during a large flare (Güdel et al. 2002).	14
Correlation between quiescent radio and X-ray luminosities of magnetically active stars (symbols) and solar flares (letters; after Benz & Güdel 1994).	15
(a) VLBA image of the dMe star UV Cet; the two radio lobes are separated by about 1.4 mas, while the best angular resolution reaches 0.7 mas. The straight line shows the orientation of the putative rotation axis, assumed to be parallel to the axis of the orbit of UV Cet around the nearby Gl 65 A. The small circle gives the photospheric diameter to size, although the precise position is unknown (after Benz et al 1998). (b) VLBA image of the Algol binary. The most likely configuration of the binary components is also drawn. The radio lobes show opposite polarity (Mutel et al 1998; reproduced with permission of the AAS.)	18
(a) Equatorial model for the magnetosphere of the young B star S1 in ρ Oph (André et al. 1988). (b) Sketch for radio emission from a global dipole consistent with the VLBI observation shown in Figure 7b (Mutel et al. 1998; reproduced with permission of the AAS.)	19
(a) Betelgeuse observed at 43 GHz. The radio photosphere of this star is resolved, with an angular resolution of 40 mas. (b) The atmospheric temperature of Betelgeuse as a function of radius, observed at different frequencies. (From Lim et al. 1998; reproduced with the permission of Nature.)	21
VLA map of the WR 147 system observed at 3.6 cm. Also shown are calculated model curves that follow the shock formed by the two-wind interaction (from Contreras & Rodríguez 1999; reproduced with the permission of the AAS).	23
Observation of the T Tau system at 6 cm with the MERLIN interferometer. Right- and left-hand circularly polarized components are shown dashed and solid, respectively. The offset of the polarized flux centroids in T Tau(S) is interpreted in terms of polarized outflows (Ray et al. 1997; reproduced with the permission of Nature.)	25